2016

Effects of Defects on the Performance of Hierarchical Honeycomb Metamaterials Realized Through Additive Manufacturing

Kazi Moshiur Rahman
South Dakota State University

EFFECTS OF DEFECTS ON THE PERFORMANCE OF HIERARCHICAL HONEYCOMB METAMATERIALS REALIZED THROUGH ADDITIVE MANUFACTURING

BY

KAZI MOSHIUR RAHMAN

A thesis submitted in partial fulfillment of the requirements for the

Master of Science

Major in Mechanical Engineering

South Dakota State University

2016

EFFECTS OF DEFECTS ON THE PERFORMANCE OF HIERARCHICAL HONEYCOMB METAMATERIALS REALIZED THROUGH ADDITIVE MANUFACTURING

This thesis is approved as a creditable and independent investigation by a candidate for the Master of Science in Mechanical Engineering degree and is acceptable for meeting the thesis requirements for this degree. Acceptance of this does not imply that the conclusions reached by the candidate are necessarily the conclusions of the major department.

Todd Letcher, Ph.D.
Thesis Advisor Date

Kurt Bassett, Ph.D.
Head, Department of Mechanical Engineering Date

Dean, Graduate School Date

I dedicate this work to my whole family for their unconditional love, faith and inspiration throughout my entire life.

ACKNOWLEDGEMENTS

I wish to express my sincere gratitude to **Dr. Todd Letcher**, my thesis advisor for his enormous support, continual encouragement and valuable advice throughout my MS thesis work. I truly feel blessed to have the opportunity to work with him throughout my entire MS degree program. I thank him for introducing me with Additive Manufacturing research. His geniality made me to ask for any help whenever needed at academic as well as personal level. His words of support during my hard days helped me to move forward. His enormous help to get financial assistance during my study meant a lot to me. I would always cherish to work with him again in future days.

I would like to thank **Dr. Zhong Hu**, graduate coordinator and my co-advisor for his valuable guidance with finite element analysis throughout my thesis work. I also acknowledge his confidence and faith in me for a graduate teaching assistantship position before starting to pursue my MS degree at South Dakota State University. It would not be a justice not to thank and acknowledge the Department of Mechanical Engineering for the financial assistance during my entire degree period.

Besides, I thank all the members of the Lab for Engineering of Additive Designs; Education and Research (LEADER) for helping me in whatever way possible. I also thank the Materials Testing and Evaluation Lab (METLAB) for all experimental research works and the University high performance research computing service for all computational research works.

Finally, I thank all of my friends and family for their endless love, faith and support in me. I am today's "ME" because of them.

TABLE OF CONTENTS

LIST OF FIGURES

LIST OF TABLES

ABSTRACT

EFFECTS OF DEFECTS ON THE PERFORMANCE OF HIERARCHICAL HONEYCOMB METAMATERIALS REALIZED THROUGH ADDITIVE MANUFACTURING

KAZI MOSHIUR RAHMAN

2016

Cellular metamaterials are of immense interest for many current engineering applications. Tailoring the structural organization of cellular structures leads to new metamaterials with superior properties providing lightweight and very strong/stiff structures. The incorporation of hierarchy to regular cellular structures enhances the properties and introduces novel tailorable metamaterials. For many complex cellular metamaterials, the only realistic manufacturing process is additive manufacturing (AM). The use of AM to manufacture large structures may lead to several types of defects during the manufacturing process, such as imperfect cell walls, irregular thickness, flawed joints, partially missing layers, and irregular elastic plastic behavior due to toolpath. It is important to understand the effect of defects on the overall performance of the structures to determine if the manufacturing defect(s) are significant enough to abort and restart the manufacturing process or whether the material can still be used in its defective state.

Honeycomb structures are often used for the high strength to weight ratio applications. These metamaterials have been studied and several models have been developed based on idealized cell structures to explain their elastic plastic behavior. However, these models do not capture real-world manufacturing defects resulting from AM. The variation of elastic plastic behavior of regular honeycomb structures with defects

has been studied, but the performance of hierarchical honeycomb structures with defects is still unknown. In this study, cell wall defects are modeled as the worst case scenario, which is entirely missing cell walls. The effects of missing cell walls are investigated to understand the elastic behavior of hierarchical honeycomb structures using finite element analysis.

Hierarchical honeycombs demonstrated more sensitivity to missing cell walls than regular honeycombs. On average, the axial elastic modulus decreased by 45% with 5.5% missing cell walls for regular honeycombs, 60% with 4% missing cell walls for first order hierarchical honeycomb and 95% with 4% missing cell walls for second order hierarchical honeycomb. The transverse elastic modulus decreased by about 45% with more than 5.5% missing cell walls for regular honeycomb, about 75% with 4% missing cell walls for first order and more than 95% with 4% missing cell walls for second order hierarchical honeycomb

CHAPTER 1 - INTRODUCTION

1.1 Introduction to cellular structures

Mechanical cellular structures are a complex interconnected network of solid struts and plates forming individual cells [1]. The structural organization of these type of structures make them unique from other structures. These structures are ubiquitous in nature. Examples of natural cellular structures are foams, honeycombs, cancellous bones, wood (Figure 1) etc. *Honeycombs* are the cellular structures with two-dimensional array of hexagonal polygons while *foams* are three-dimensional cellular structures with polyhedral unit cells.

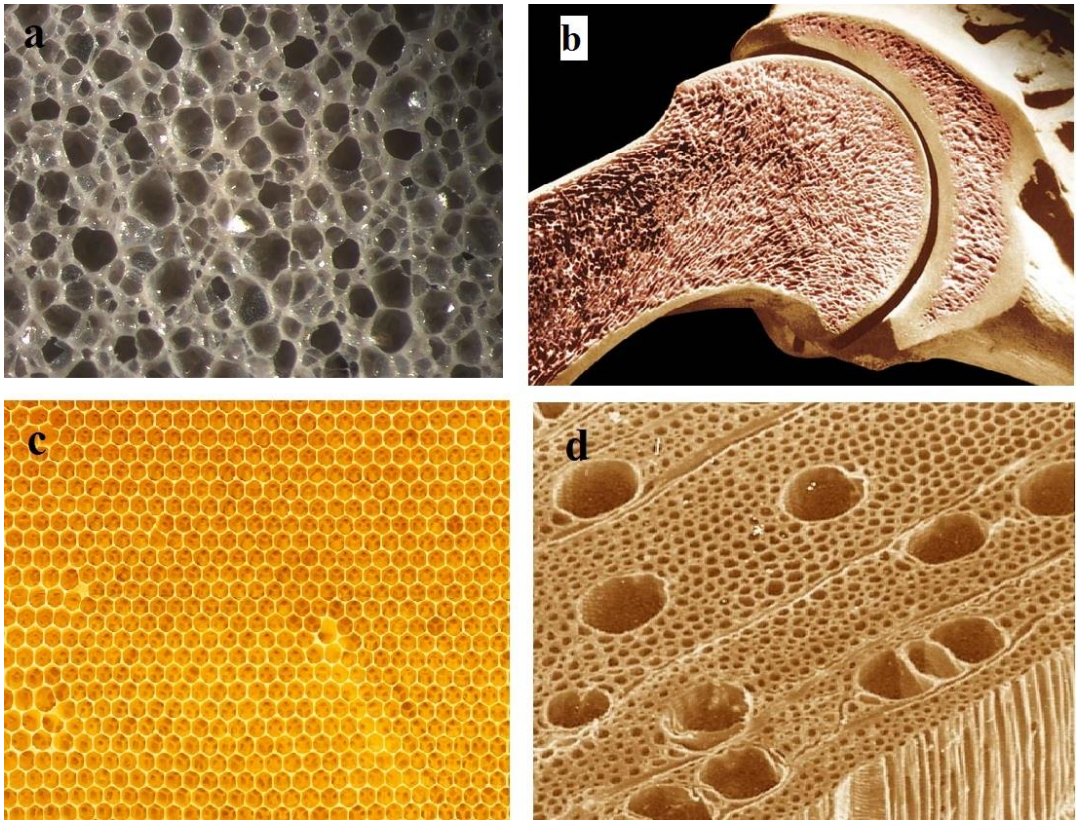

Figure 1: Natural cellular structures (a) foam [2] (b) cancellous bone [3] (c) honeycomb [4] (d) wood [5]

The relative density of the cellular structure, ρ^*/ρ_s (where ρ^* is the density of the cellular structure and ρ_s is the density of the solid material from which the cellular structure is made), is the most important feature that makes it different from regular solids. Cellular foams with relative density as low as 0.001 are possible. Polymeric foams used in different applications such as packaging, insulation and cushioning have relative densities ranging in between 0.05 and 0.2. A commonly known material, cork, has a relative density of about 0.1[1]. The cell wall thickness of cellular structures increases with the increase of the relative density. When the relative density is above about 0.3, the cellular structures have a transition to regular solids containing isolated pores and are no longer considered cellular structures. If the solid of which the cellular structures is made is contained in the cell edges only (so that the cells connect through open faces), the cellular structure is called open-celled (Figure 2(a)). When the faces are solid too, it is called as closed-celled (Figure 2(b)). Some natural cellular structures have both open-celled and closed-celled faces.

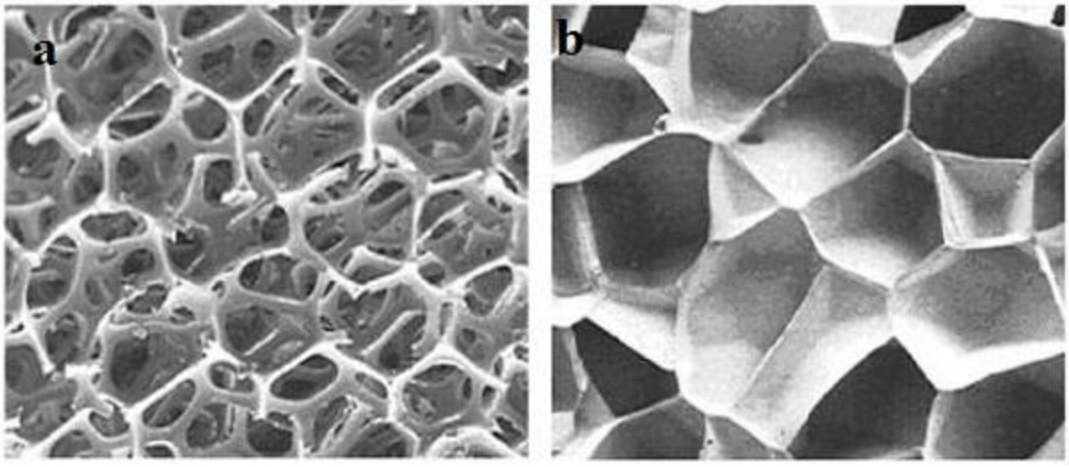

Figure 2: Cellular foams (a) open-cell (b) closed-cell [6]

Cellular structures offer a broad range of effective mechanical properties with the organization of the cells. The low density feature of cellular structures inspires researchers and engineers to design lightweight and stiff applications such as sandwich panels. In addition, cellular structures can be used for variety of cushioning applications such as elastomeric foams due to their low stiffness. Cellular foams are a smart choice for energy absorbing applications too due their low strength and large compressive strains. Furthermore, the low thermal conductivity feature of cellular structures makes them a good and reliable candidate for thermal insulation applications.

1.2 Applications of Cellular structures

There are four major areas of applications of cellular structures with some other smaller and growing areas. The four areas are: thermal insulation, structural use, packaging and buoyancy [1].

The largest area of application of polymeric and glass foams is insulation. Products starting from disposable coffee cups to booster rockets for the space shuttle use the low thermal conductivity foams for insulation purpose. The low thermal conductivity feature of cellular structures is also exploited by modern buildings, refrigerated trucks, railway cars, and even ships carrying liquid natural gas. Glass foams can be used instead of polymeric foams in buildings (to avoid any damage from fire), in pipes and roofs for very long life. Foams have very low thermal mass which helps reducing the amount of refrigerant needed to cool the insulation itself. Similarly, the lower thermal mass leads to higher efficiency at higher temperature applications such as furnaces and kilns. A large

part of the energy dissipated in furnaces and kilns is utilized to raise the temperature of the structure to the operating level; the lower the thermal mass, the higher the efficiency.

Natural cellular structures such as woods, cancellous bones, corals etc. support large static and cyclic loads over a long period of time. The mechanics of cancellous bones can help to understand various bone diseases and design materials to replace damaged bones. Currently, designed foams and honeycombs are used in structural applications extensively. Honeycomb sandwich panels used in various structural safety or in modern aircrafts provide enormous bending stiffness and strength to the structure. Sandwich panels are also popular in weight critical applications such as spacecraft, yachts and portable buildings etc.

One of the major use of cellular structure is in packaging. An effective package must absorb the energy from impact loading without causing any damage to the products. Foams can undergo large compressive strains at almost constant stress, hence, can easily absorb large amount of impact loading without generating high stresses. Moreover, the strength of foams can be adjusted over a wide range by controlling the relative density.

Cellular structures like foams have extensive use in marine buoyancy. Floating structures are supported by various closed-cell plastic foams. There are several advantages of using foams in buoyancy applications. Foams have large damage tolerance compared to floatation bags or chambers, can retain buoyancy even when subjected to major damage, are unaffected by extended emersion in the water and are not susceptive to rustiness or corrosiveness. Cellular sandwich panels are also used to make the deck and hull of the boats providing structural rigidity as well as buoyancy.

Cellular structures have other uses such as filters (air filters, metal casting filters, molecular membrane filters etc.), carriers (carriers of dyes, inks, lubricants, carriers of catalysts etc.), dampeners (sound wave dampeners in ceilings and walls) etc.

1.3 Introduction to Hierarchy

Cellular structures are of immense interest in engineering applications. The need for lightweight and stiff structures leads researchers and engineers to develop new cellular structures inspired by nature. Incorporation of structural hierarchy in cellular structures at different length scales is a novel way to tailor mechanical properties such as stiffness [7], toughness [8], strength [9], auxeticity (negative Poisson's ratio materials) [10] etc. Hierarchical structures are obtained by adding material to places where high stress is concentrated due to impact loading. The main objective of introducing hierarchy to cellular structure is to enhance the mechanical behavior without increasing the weight of the structure. Studies have shown that increasing the level of hierarchy leads to lighter weight structure with better performance [7-10]. In the current study, hierarchy of honeycomb structures will be explored.

Structural hierarchy into honeycomb structures have been studied extensively. Several different techniques have been explored to incorporate hierarchy into honeycomb structures. Mousanezhad et al [11] proposed a spiderweb hierarchical fractal-like honeycomb structure (Figure 3). The isotropic in-plane elastic moduli (Young's modulus and Poisson's ratio) of these structures are controlled by dimension ratios (γ_1 and γ_2 as shown in Figure 3) in the hierarchical pattern of the honeycomb. Moreover, these spiderweb honeycombs exhibit auxetic behavior depending upon the dimension ratios.

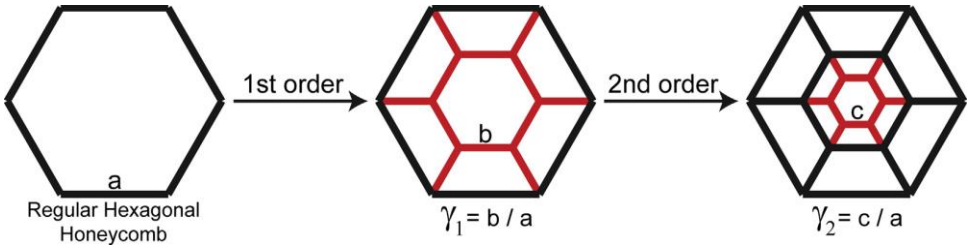

Figure 3: Evolution of the unit cell in a regular hexagonal honeycomb into first and second order spiderweb honeycombs proposed by Mousanezhad et al.

Fan et al [12] investigated the hierarchical honeycomb made up of sandwich struts (Figure 4). Stiffness, buckling strength, plastic collapse strength, brittle failure strength, and the fracture toughness was analytically determined. The authors also discussed the enhancement mechanism of 2nd order hierarchical honeycomb analytically. According to their analysis, sandwich struts have proven to enhance the buckling strength of 2nd order hierarchical honeycomb.

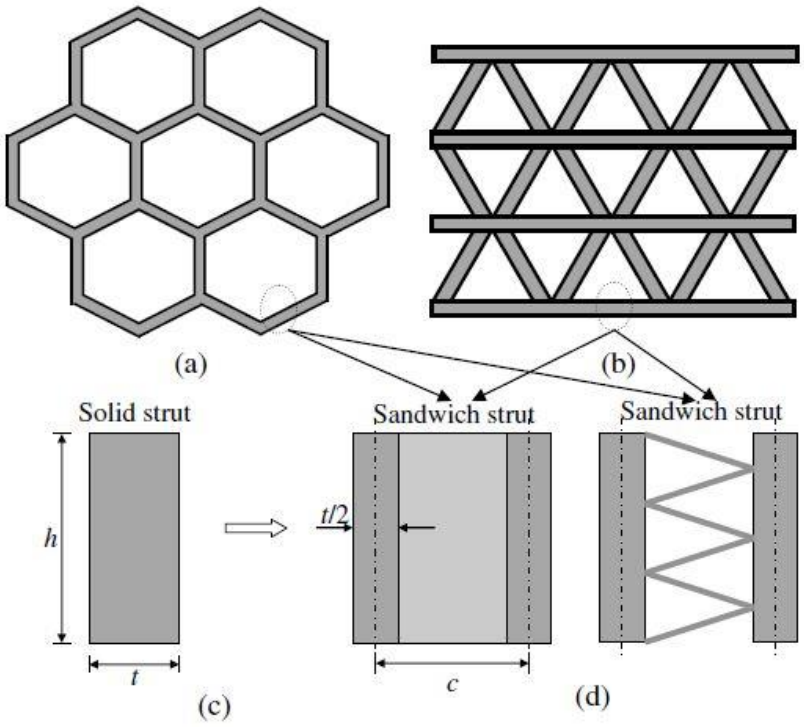

Figure 4: Hierarchical honeycomb suggested by Fan et al.

Kooistra et al [13] suggested a hierarchical honeycomb where the homogeneous cell walls are replaced by trusses (Figure 5). Analytical expressions were derived for the compressive and shear collapse strengths and used that to construct collapse mechanism maps for second order trusses. Collapse mechanism maps were used to select the geometries of second order trusses that maximize the collapse strength for a given mass. Analytical predictions were verified experimentally and found that the strength of second order truss is about ten times greater than the first order truss of same relative density. It was also determined that increasing the level of structural hierarchy yields no enhancements in the stiffness. In fact, the stiffness to weight ratio of the first order core is slightly greater than its second order counterpart suggesting that the hierarchical construction has applications in strength limited applications.

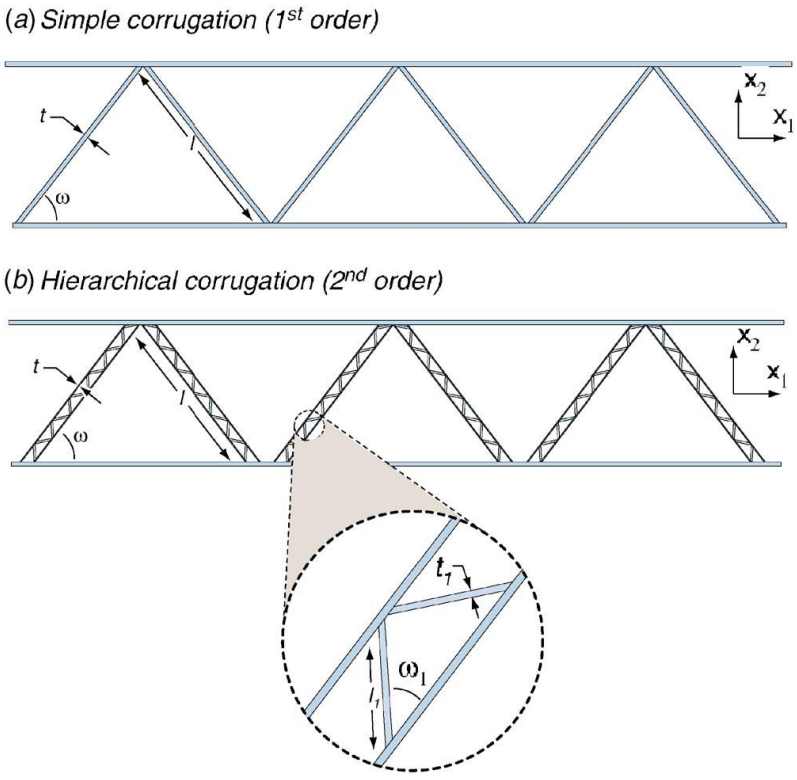

Figure 5: Hierarchical structure suggested by Kooistra et al.

Taylor et al [14] suggested adding hierarchical sub-structures to honeycombs (Figure 6). Elastic properties and structural hierarchy in honeycombs were investigated and the effects of adding hierarchy into a range of honeycombs, with hexagonal, triangular or square geometry super and sub-structure cells was explored. It was determined that the introduction of a hierarchical sub-structure into a honeycomb has a deleterious effect upon the in-plane density specific elastic modulus vs a conventional non-hierarchical version in most cases.

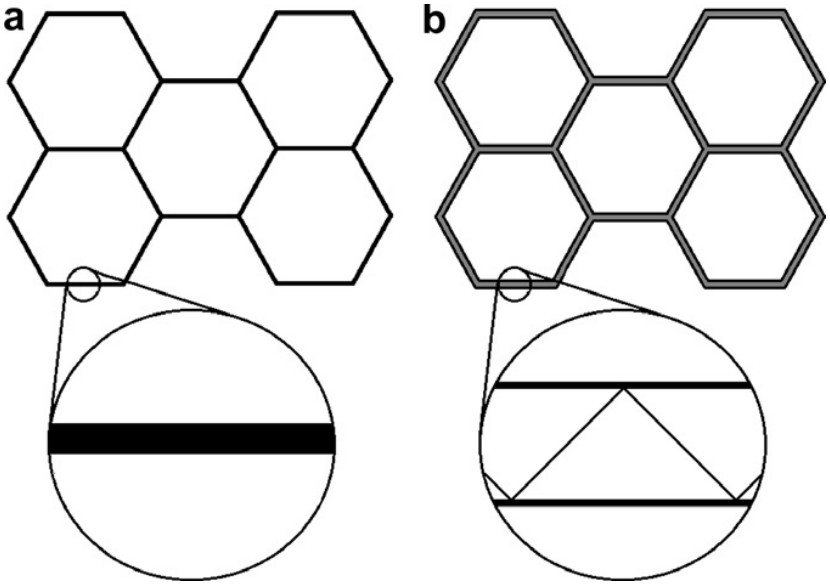

Figure 6: Hierarchical honeycomb suggested by Taylor et al (a) first order hierarchy (b) second order hierarchy

Dag Lukkassen [15] presented a reiterated honeycomb structure (Figure 7) with different micro-levels. These micro-levels are formed by dividing each edge of hexagonal honeycomb into three equal parts and creating an interior with six smaller hexagons surrounding another hexagon. It was determined that the upper and lower bounds of corresponding effective properties using homogenization theory. Higher levels of hierarchy can be obtained by repeating the same process.

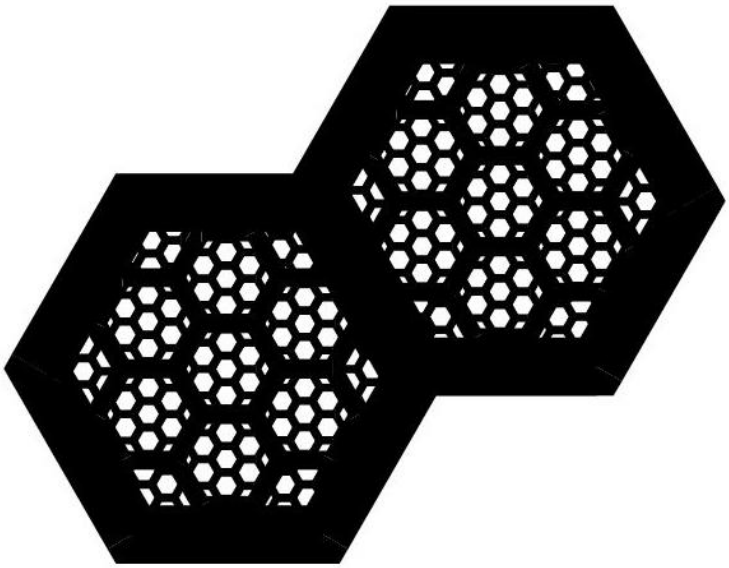

Figure 7: Reiterated hierarchical honeycomb structure by Dag Lukkassen

Ajdari et al [7] presented a different type of hierarchical honeycomb by changing each three edge vertex of a regular hexagonal honeycomb lattice by adding another smaller hexagon to get first level of hierarchy. The second level of hierarchy is created by adding another smaller hexagon at each three edge vertex of the hexagons added for the first order hierarchy. For the hierarchical cases, the overall density of the honeycomb is held constant to the parent structure (zeroth order or regular) by reducing the thickness of the cell wall in the first and second order structures.

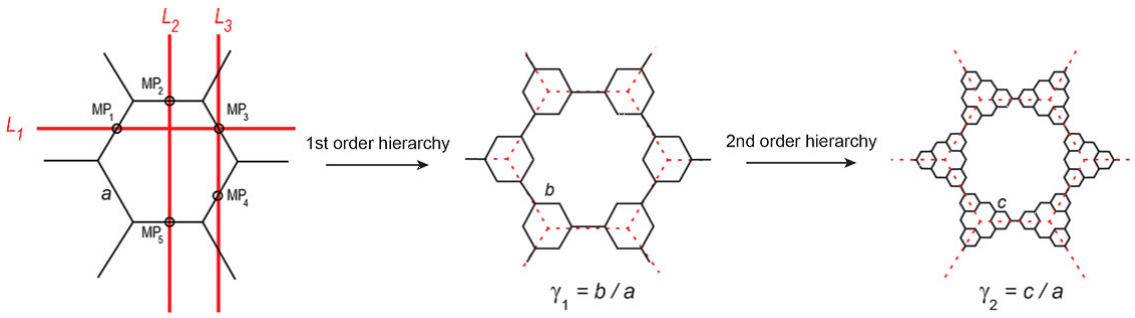

Figure 8: Hierarchical honeycomb structure introduced by Ajdari et al

The isotropic in-plane elastic properties (effective elastic modulus and Poisson's ratio) of this structure are controlled by the dimension ratios (γ_1 and γ_2 as shown in the Figure 8) for different hierarchical orders. It was determined that a relatively broad range of elastic properties and behavior can be achieved by tailoring the structural organization of hierarchical honeycombs, specifically changing the dimension ratios. These hierarchical honeycombs of first and second order can be up to 2.0 and 3.5 times stiffer respectively than regular honeycomb at the same mass (i.e., same overall average density).

Mousanezhad et al [10] used the hierarchical structure introduced by Ajdari et al to design a new class of 2D auxetic metamaterials capable of exhibiting auxeticity over a wide range of applied compressive strains. It was shown that higher orders of hierarchy can lead to more auxetic response from the structure. This provides new insights into designing energy absorbing materials and tunable membrane filters.

Oftadeh et al [16] constructed fractal-appearing hierarchical honeycomb up to several orders (Figure 9). Mechanical properties of the structure after different orders of iteration were optimized. It was determined that the optimal structure is self-similar but requires higher order of hierarchy as the density deceases. The effective elastic modulus of the hierarchical structures increase with the increase of orders while preserving the structural density.

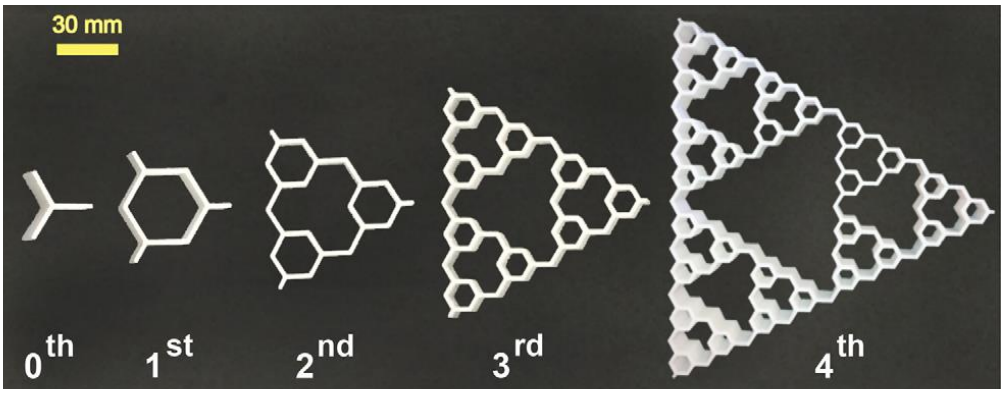

Figure 9: Unit cell of regular to fourth order hierarchical honeycombs by Oftadeh et al

1.4 Evolution and Mechanics of Hierarchical Honeycomb

The hierarchical honeycomb studied in present work was first introduced by Ajdari et al [7]. The transverse stiffness and strength of honeycomb structures are governed by the cell wall bending and the relative density of the structures [1]. When subjected to uniaxial loading, the maximum bending happens to be at the corners of the cells. Moving materials from the middle part of the cells to the corners can potentially increase the stiffness and strength [17]. The three-edge vertices of the regular honeycomb are replaced with smaller hexagons to create first level of hierarchy. Again, the three-edge vertices of the first order hierarchy are replaced by smaller hexagons to create second level of hierarchy. Repeating this process with smaller hexagons leads to higher level of hierarchy. Figure 10 shows the evolution of first order and second order hierarchy from regular honeycomb structure.

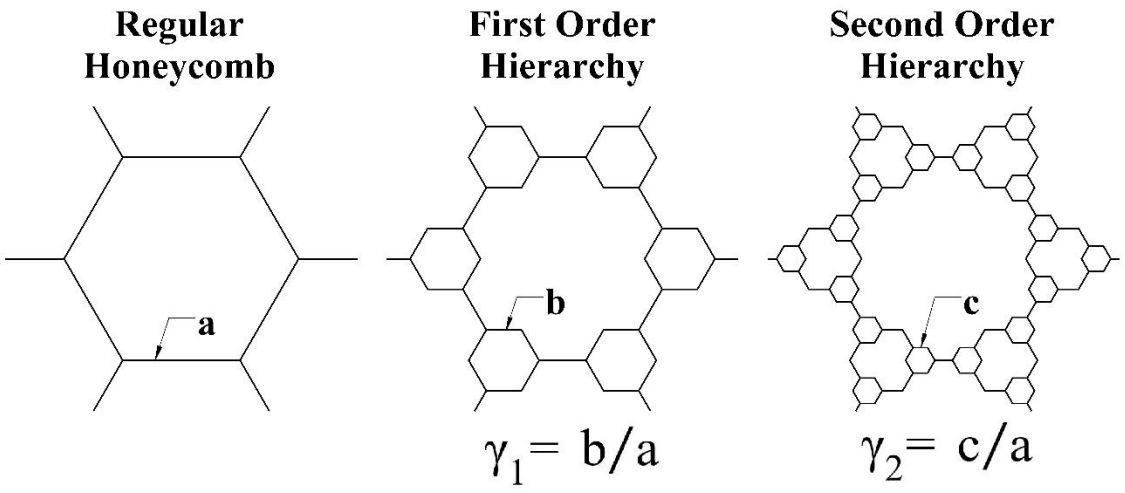

Figure 10: Evolution of Hierarchical Honeycomb

The hierarchical honeycomb structures can be defined by the dimension ratios γ_1 and γ_2, which represent the ratio of the smaller honeycomb edge length to the parent honeycomb edge length (zeroth order or regular honeycomb). These ratios are better understood by Figure 10, where $\gamma_1 = b/a$ and $\gamma_2 = c/a$. The following geometric constraints must be maintained:

For first order hierarchy,

$$0 \leq b \leq \frac{a}{2} \tag{1}$$

$$0 \leq \gamma_1 \leq 0.50 \tag{2}$$

For second order hierarchy,

$$0 \leq c \leq b \tag{3}$$

$$c \leq \frac{a}{2} - b \tag{4}$$

The density of the structure normalized by the parent material density is given by,

$$\rho = \frac{2}{\sqrt{3}}(1 + 2\gamma_1 + 6\gamma_2)\left(\frac{t}{a}\right) \quad (5)$$

Where, t = thickness of the cell walls.

For regular honeycomb, $\gamma_2, \gamma_1 = 0$ and the relative density term decreases to $\rho = \frac{2}{\sqrt{3}}\left(\frac{t}{a}\right)$, for first order hierarchical honeycomb, $\gamma_2 = 0$, and the relative density term decreases to $\rho = \frac{2}{\sqrt{3}}(1 + 2\gamma_1)\left(\frac{t}{a}\right)$. To maintain a fixed relative density, t/a must be decreased as γ_2, and γ_1 are increased. For any specific length of regular honeycomb cell wall (i.e., "a"), the thickness of corresponding first order and second order hierarchical honeycomb must be adjusted to maintain constant relative density.

Regular hexagonal honeycomb cell walls bend and deform linearly when subjected to in-plane stresses (X_1 and X_2 direction in Figure 11). Under in-plane compressive loading, the stiffness and strength are lowest as the cell walls respond with bending. The out of plane (X_3 direction in Figure 11) stiffness and strength are highest because they require axial deformation. Regular hexagonal honeycombs have uniform cell wall edge length with 120° intercellular angles. Regular honeycombs with uniform cell wall thickness have isotropic in-plane properties.

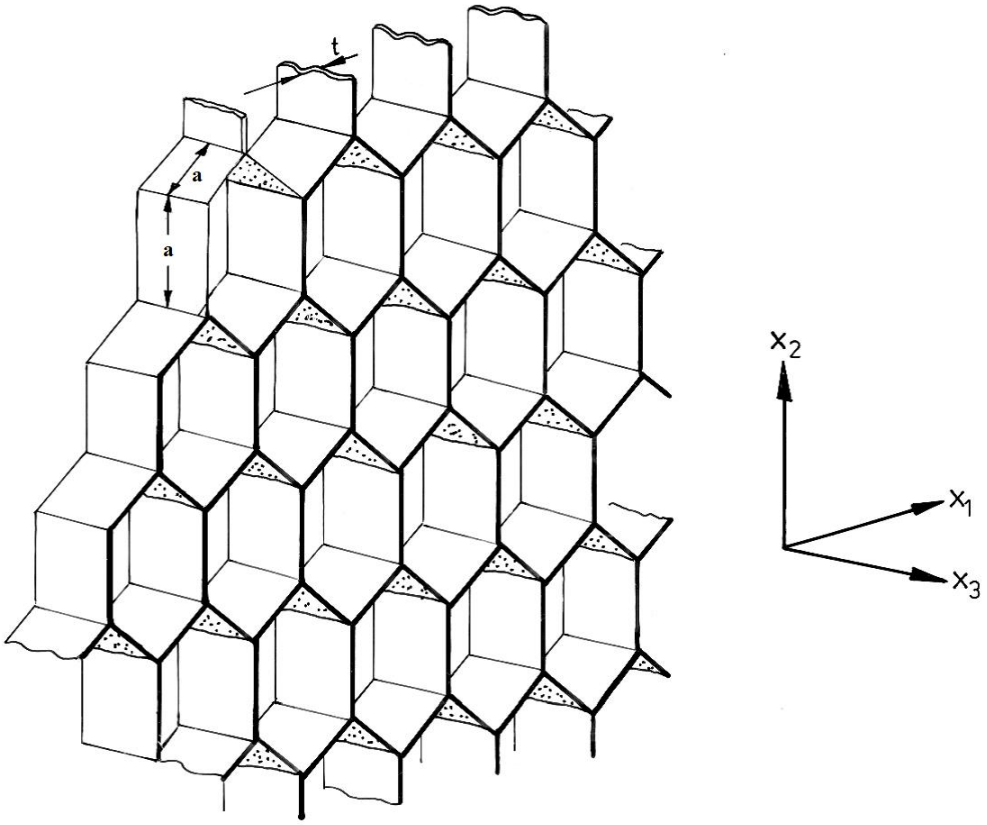

Figure 11: A hexagonal honeycomb structure (in-plane loading in X_1-X_2 direction, out of plane loading in X_3 direction) (adapted from [1])

If a stress of σ_1 is applied parallel to X_1 direction, the cell walls start to bend (see Figure 12). The component of D parallel to X_2 must be zero for equilibrium. The cell wall (thickness t, cell wall length a, depth b and Young's Modulus E_s) bending moment M can be written as,

$$M = \frac{Pa \sin\theta}{2} \tag{6}$$

Where "P" is given by,

$$P = \sigma_1(a + a \sin\theta)b \tag{7}$$

The deflection of the cell wall can written using standard beam theory as,

$$\delta = \frac{Pa^3 \sin\theta}{12E_s I} \tag{8}$$

Where "I" is the second moment of inertia of the cell wall and is equal to $bt^3/12$.

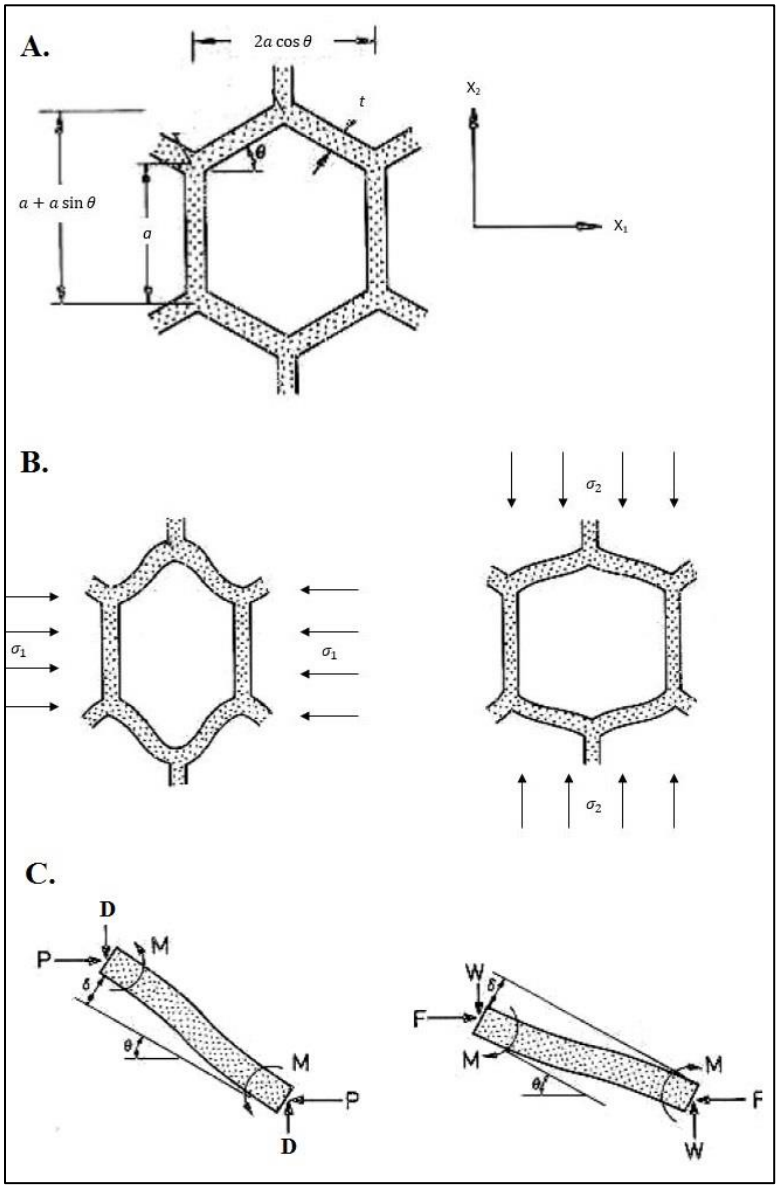

Figure 12: Unit cell of regular hexagonal honeycomb A. Undeformed cell B. and C. Bending deformation in X_1 and X_2 direction (adapted from [1])

The strain due to the stress σ_1 is,

$$\varepsilon_1 = \frac{\delta \sin\theta}{a\cos\theta} = \frac{\sigma_1(a + a\sin\theta)ba^2 sin^2\theta}{12E_s I\cos\theta} \quad (9)$$

Therefore, the Young's modulus parallel to X_1 is,

$$E_1 = \sigma_1/\varepsilon_1 \quad (10)$$

Which ultimately gives,

$$\frac{E_1}{E_s} = \left(\frac{t}{a}\right)^3 \frac{\cos\theta}{(1+\sin\theta)sin^2\theta} \quad (11)$$

For, regular honeycomb with uniform thickness,

$$\frac{E_1}{E_s} = 2.31\left(\frac{t}{a}\right)^3 \quad (12)$$

When a stress σ_2 is applied from X_2, the cell wall bending occurs as shown in Figure 12 B and C. For equilibrium, F = 0 and $W = \sigma_2 ab\cos\theta$. The bending moment is,

$$M = \frac{Wa\cos\theta}{2} \quad (13)$$

The deflection of the wall is given by,

$$\delta = \frac{Wl^3\cos\theta}{12E_s I} \quad (14)$$

The strain is,

$$\varepsilon_2 = \frac{\delta\cos\theta}{a + a\sin\theta} = \frac{\sigma_2 ba^4 cos^3\theta}{12E_s I(a + a\sin\theta)} \quad (15)$$

Therefore, the Young's modulus parallel to X_2 is,

$$E_2 = \sigma_2/\varepsilon_2 \quad (16)$$

Which gives,

$$\frac{E_2}{E_s} = \left(\frac{t}{a}\right)^3 \frac{(1+\sin\theta)}{cos^3\theta} \tag{17}$$

For, regular honeycomb with uniform thickness,

$$\frac{E_2}{E_s} = 2.31\left(\frac{t}{a}\right)^3 \tag{18}$$

Equation 12 and 18 indicate that, hexagonal honeycomb with uniform cell wall length and uniform thickness, are isotropic in nature.

The first order and second order hierarchical honeycomb structure mechanics was first analytically solved by Ajdari et al [7]. For first order hierarchy, an external negative Y direction force F is applied to point 4 (Figure 13A) which is the midpoint of the cell edge. The cell wall bending moments M_1 and M_2 due to the force on point 1 and 2 respectively. The reactions N_1 and N_2 are on point 1 and 2 respectively in the positive Y direction.

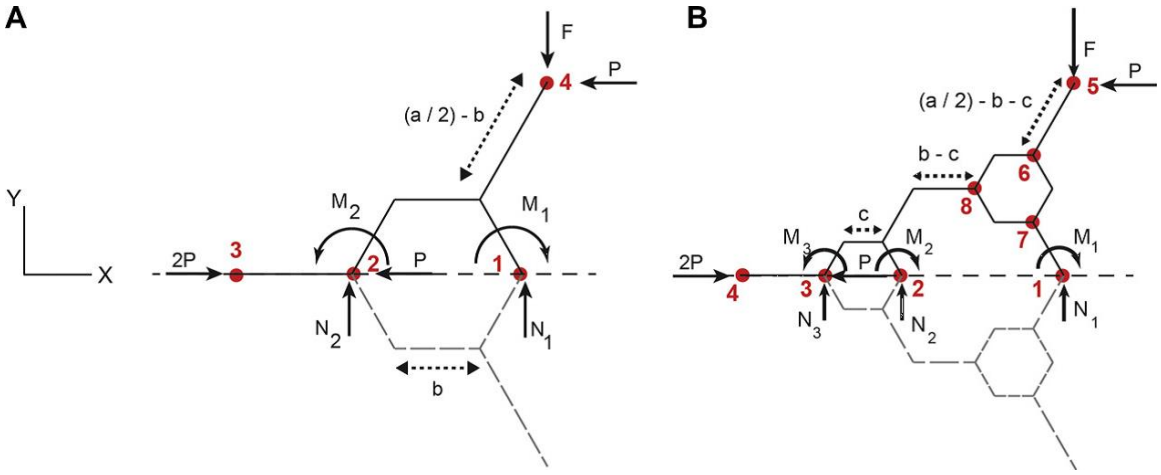

Figure 13: Mechanics of hierarchical honeycomb analytical approach. A. First order hierarchy. B. Second order hierarchy [7]

Using equilibrium equations, Ajdari et al found the Young's modulus of first order hierarchical honeycomb as,

$$\frac{E}{E_s} = \left(\frac{t}{a}\right)^3 f(\gamma_1) \tag{19}$$

Where, $f(\gamma_1) = \sqrt{3}/(0.75 - 3.525\gamma_1 + 3.6\gamma_1^2 + 2.9\gamma_1^3)$

For second order hierarchy, same approach has been taken. An external negative Y direction force F is applied at point 5 (Figure 13B). The bending moments M_1, M_2 and M_3 occurs at point 1, 2 and 3 respectively. The reaction forces are N_1, N_2 and N3 at points 1, 2 and 3 respectively. Using equilibrium equations, the Young's modulus can be found as,

$$\frac{E}{E_s} = \left(\frac{t}{a}\right)^3 f(\gamma_1, \xi) \tag{20}$$

Where, $\xi = \gamma_2/\gamma_1$ and $f(\gamma_1, \xi) = N_4(\xi)/(\gamma_1^3 D_7(\xi) + \gamma_1^2 D_6(\xi) + \gamma_1 D_5(\xi) + D_4(\xi))$

$N_4(\xi) = 29.62 - 54.26\xi + 31.75\xi^2 - 4.73\xi^3 - \xi^4$

$D_7(\xi) = 49.64 - 609.01\xi + 862.56\xi^2 - 195.50\xi^3 - 270.14\xi^4 + 159.95\xi^5 - 18.13\xi^6 - 2.20\xi^7$

$D_6(\xi) = 61.73 + 310.43\xi - 662.32\xi^2 + 334.12\xi^3 + 9.70\xi^4 - 29.38\xi^5 - 1.88\xi^6$

$D_5(\xi) = 60.43 + 12.80\xi + 123.22\xi^2 - 108.06\xi^3 + 20.50\xi^4 + 3.90\xi^5$

$D_4(\xi) = 12.80 - 323.46\xi + 13.74\xi^2 + 2.04\xi^3 - 0.43\xi^4$

1.5 Introduction to Additive Manufacturing

Additive manufacturing (AM), otherwise known as 3D printing, is a process of manufacturing objects layer by layer, as opposed to conventional subtractive manufacturing technologies. AM has been described by many as the beginning of the "next industrial revolution", and as such, AM processes have gained popularity in the fields of aerospace [18], automotive [19], biomedical [20], energy [21] and other fields with the advancement of superior technologies. Today, plastics [22-24], metals [25], ceramics [26] and even glass [27] are being used for prototyping as well as fabricating functional parts through AM. Although there are several AM process, the basic principle is same for all. In a generic AM process the model describing the full geometry of an object is initially created using a three-dimensional CAD (Computer Aided Design) software (i.e., SolidWorks®, Pro/Engineer® etc.). The model is then converted to an appropriate format (usually Stereolithography, otherwise known as STL) and taken to a software usually called a 'slicer' for preprocessing specifying build parameters (material constraints, layer thickness, number of layers/shells etc.). The slicer software converts the model into a series of cross-sectional layers (two-dimensional layers) and generates instructions for the AM machine (i.e., 3D printer) to fabricate the object. The processed file is then taken to the AM machine. The AM machine then fabricates the object according to the instructions by feeding materials in successive layers. Perhaps the most intriguing aspect of AM is that if any object geometry can be defined through a CAD data, AM technologies can make that object regardless of the geometrical complexity.

1.6 Additive Manufacturing Technologies

Much of the AM field has advanced very rapidly in recent years, including both hardware and software advancements. Many AM processes have been invented since the inception of the technology. The differences of various AM processes are the way successive layers are added to make the objects and the materials used to make the objects. Currently available AM processes include Fused Filament Fabrication (FFF), Stereolithography (SLA), Selective Laser Sintering (SLS), and Electron Beam Melting (EBM), Jetting etc.

1.6.1 Fused Filament Fabrication

Fused Filament Fabrication (FFF) AM technology is also known as Fused Deposition Modeling (FDM). Fused Deposition Modeling and it's abbreviation FDM are trademarked by Stratasys Inc., one of the major market players in the field of additive manufacturing technology. In FFF (or FDM), a spool of filament of a certain material (usually thermoplastic or wax) is pushed through an extrusion nozzle. The nozzle is heated to a higher temperature to melt (or soften) the material and the melted material is deposited as necessary to build each layer. Stepper motors or servo motors are usually used to aid the movement of the extruder. The extruder moves horizontally (in reference to the build plate), in the x-y plane to deposit the material on the build platform. After the entire layer has been created, the build plate moves in the z direction to allow for a new layer to be deposited on top of the previous layer. The part is created using the bottom up approach. Depending on the design to be manufactured, support material may be required to create overhang sections of the object. Support materials can be either the same material with the same extruder or any soluble material with another extruder. Figure 14 shows a generic

illustration of a Fused Filament Fabrication Process. Materials currently available for FFF include but not limited to Acrylonitrile Butadiene Styrene (ABS), Polylactic acid (PLA), Polycarbonate (PC), Polystyrene (PS), Polyether Etherketone (PEEK) etc.

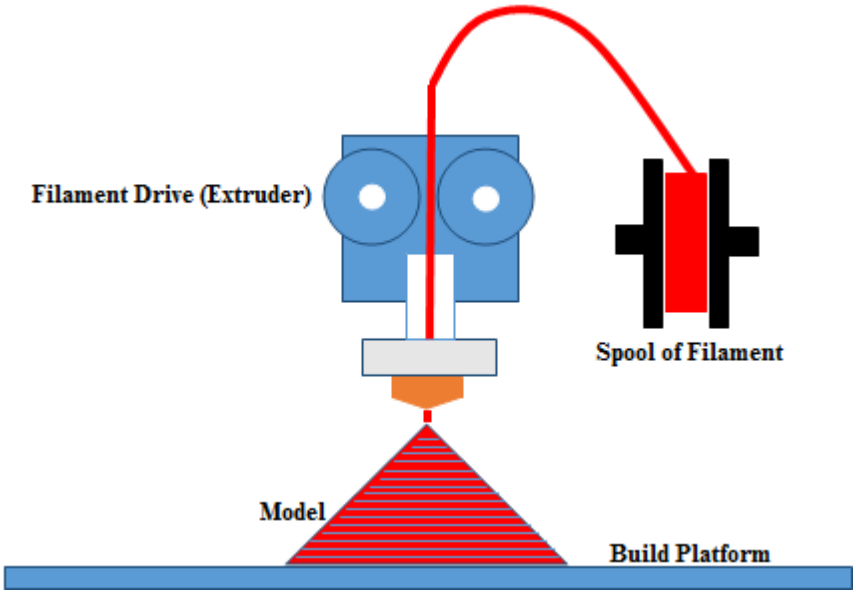

Figure 14: Fused Filament Fabrication process illustration

1.6.2 Stereolithography

Stereolithography (often called as SLA) is a popular AM process and is usually considered the first 3d printing technology. This AM process uses photopolymer resin as the manufacturing/prototyping material. An ultraviolet (UV) laser is focused on a bath of photopolymer resin to cure and solidify it producing a layer of the object [28]. The solid layer and the support platform are then lowered by a distance just to accommodate another layer and the process is repeated until a complete desired object is made. After all the layers are cured and solidified, the platform is raised and the solid polymer emerges from the resin bath. Figure 15 [29] shows a schematic of stereolithography process.

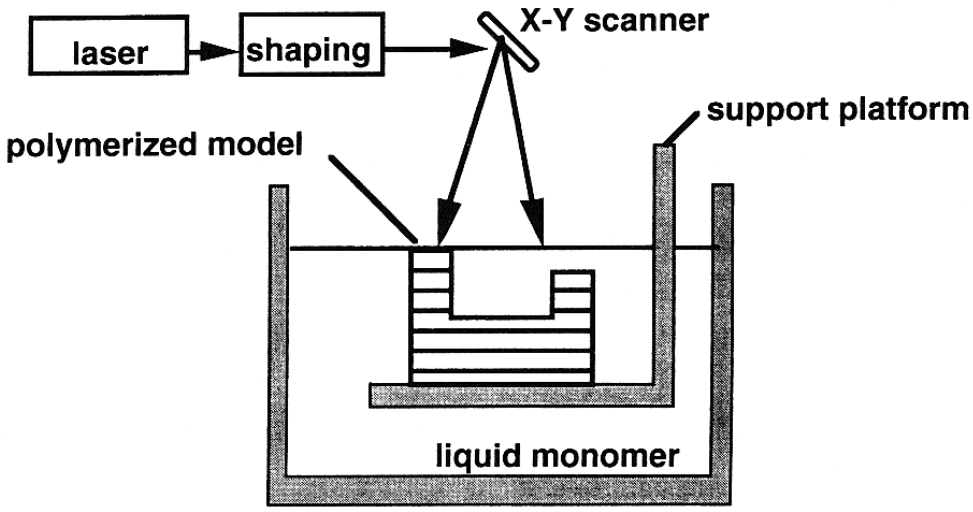

Figure 15: Schematic of Stereolithography

1.6.3 Selective Laser Sintering

Selective Laser Sintering (SLS) is similar to stereolithography (SLA), but uses powder instead of photopolymer resin as the raw material. In this process, a layer of powder is deposited on a support platform and levelled by a rolling device. A powerful laser beam is then used to selectively fuse the powder to make one layer of the object. The support platform is lowered to accommodate the next layer and another layer of powder is deposited on the previous layer. The process continues until the whole object is fabricated. SLS process is shown schematically in Figure 16 [30].

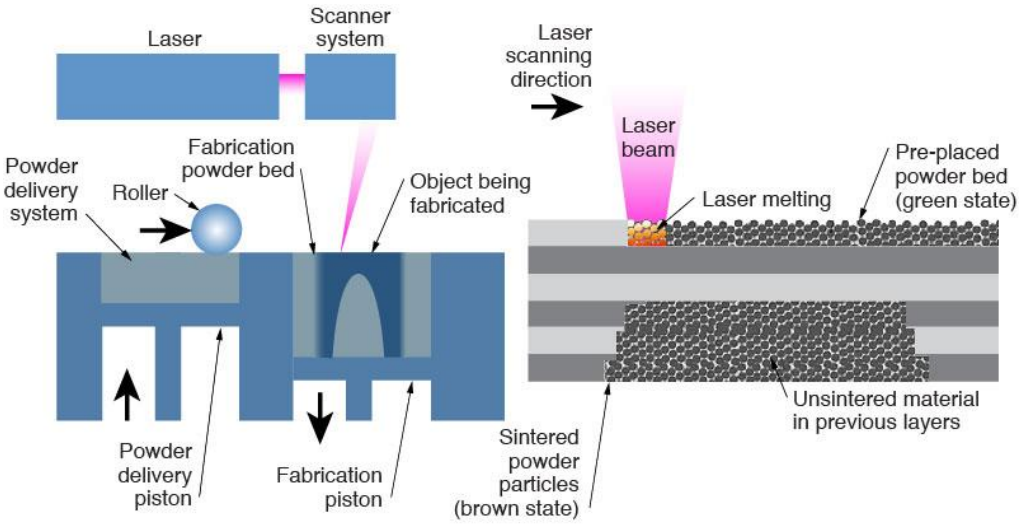

Figure 16: Selective Laser Sintering process

In the SLS process, fabricating a part with overhang does not require any additional support because the sintered part is surrounded by non-sintered powder all the time. Currently available SLS materials include polymers such as polystyrene and nylon, and metals such as steel, titanium, and aluminum.

1.6.4 Electron Beam Melting

Electron beam melting (EBM) process is an AM process for fabrication of metal parts. This process is similar to SLS, but uses an electron beam powered by a high voltage, typically 30 to 60 KV. EBM parts are built inside a vacuum chamber to avoid any energy loss due to the collision between the fast moving electron beam and air/gas molecules [31]. Figure 17 [32] shows a schematic of Electron Beam Melting process

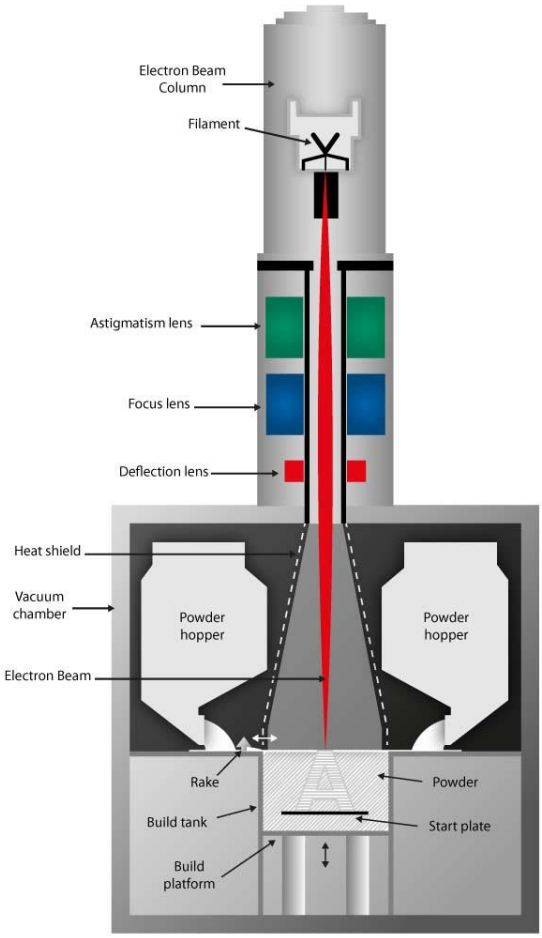

Figure 17: schematic of Electron Beam Melting process

This process can build near-net-shape parts with less raw material and finishing requirement [33]. Titanium alloys are widely used materials for EBM process.

1.6.5 Jetting

There are two AM process using jetting technique namely binder jetting and material jetting. In binder jetting, a binder is jetted and selectively sprayed into a powder bed to fuse and make a layer of the desired object. The bed is lowered and levelled by a roller for the subsequent layer to be formed and fused. Like the SLS process, binder jetting also doesn't require any provision for support material. Figure 18 [34] shows a schematic of binder jetting process.

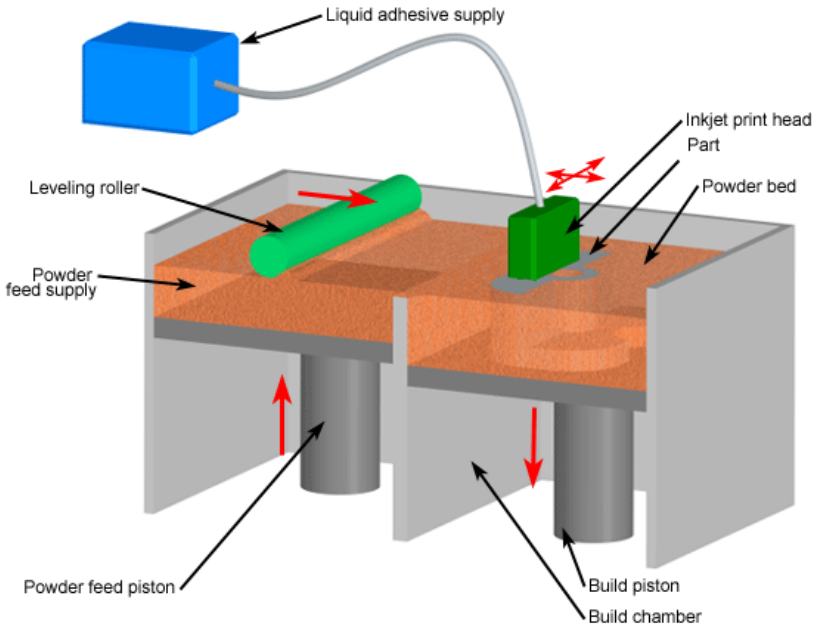

Figure 18: Binder jetting AM process

In material jetting, the build material (usually a liquid photopolymer) is selectively jetted and cured by a UV light after each layer is deposited. Support materials, if needed, can be jetted from a different jet head. This jetting process also allows to build multi-material object where each material is jetted from individual jet head. Parts made with material jetting technique tend to be very accurate and smooth. Figure 19 [35] shows a schematic of material jetting process.

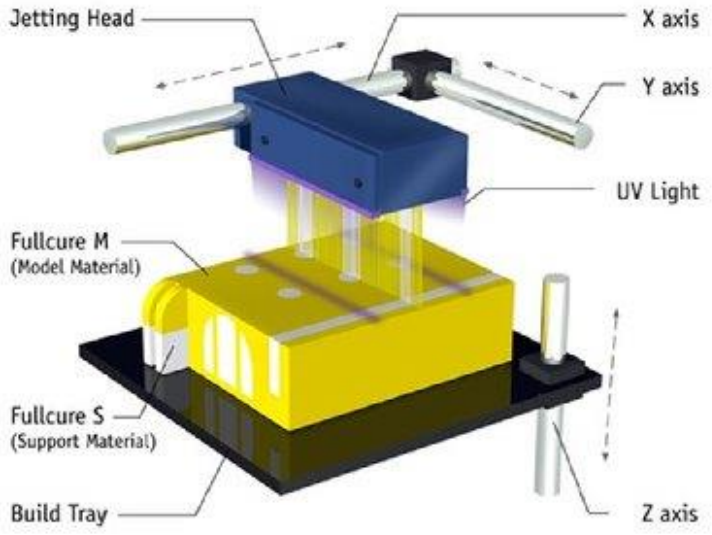

Figure 19: Material jetting AM process

1.7 Motivation of Present Work

One of the most convenient and in many cases the only way to prototype/manufacture complex cellular structures like hierarchical honeycomb is Additive manufacturing (AM). Like natural cellular materials, microstructural/macrostructural variations (i.e. imperfections and inhomogeneities) are very common in AM processes. Manufacturing/prototyping complex cellular structures through AM processes may lead to several types of defects such as missing/broken cell walls, irregular thickness, flawed joints, missing (partial) layers, filled cells and irregular elastic plastic behavior due to toolpath depending upon the process being used to manufacture/prototype. As discussed earlier, hierarchical honeycomb cellular structures are of immense importance in the fields of thermal insulation, structural safety, packaging and many others. It would be beneficial to understand the effect of defects on the overall performance of the structure to determine if the manufacturing defect(s) are significant enough to abort and restart or whether the material can still be used.

1.8 Previous works on Defects

Microstructural/macrostructural variability of regular hexagonal honeycomb has been studied extensively. Prakash et al [35] studied the macroscopic response of two-dimensional hexagonal honeycomb structures with localized filled cells and broken cell walls. It was concluded that inclusion (i.e. filled cells) stiffens the neighboring cells whereas removal of cell walls should trigger collapse of neighboring cells. Ajdari et al [36] investigated the effect of randomly missing cell walls and randomly filled cell walls on the elastic-plastic behavior of regular and voronoi honeycomb. Finite element analysis showed that the elastic modulus of regular honeycomb decreased by more than 45% with 7% missing cell walls while the it increased by 11% with 5% filled cells. The yield strength decreased by more than 60% with 10% missing cell walls. The effect was much more sensitive for voronoi structures. Silva and Gibson [37] analyzed the effects of non-periodic microstructure and defects on the compressive behavior of two-dimensional voronoi honeycombs. The analysis showed that voronoi honeycombs were approximately 30% weaker than the periodic honeycomb of same density. Also, a 10% reduction of density due to defects caused 60% reduction in the compressive strength of honeycomb.

Nakamoto et al [38] investigated the impact behavior of honeycomb structures with rigid inclusions through the finite element method. Normalized mean stress, densification strain and absorbed energy per unit volume are dependent on the fraction of inclusions. These entities increased linearly with the increase of volume fraction of inclusions. Their finite element analysis showed that honeycomb models with inclusions have more energy

absorbing capability than models without inclusions and it was highest from 10% to 20% inclusions.

Wang et al [39] investigated the effect of missing or fractured cell walls on in-plane effective stiffness and strength of square and triangular metal honeycomb. It was determined that triangular cell honeycombs exhibit more gradual reduction of properties than square and hexagonal honeycombs, and retain residual stiffness and strength even when the missing cell walls approaches 30%.

Zhang et al [40] explored the in-plane dynamic crushing behavior of honeycombs with defects in the form of random missing cell walls. Numerical results showed that the dynamic performance of honeycombs is very sensitive to defect locations, specifically under low and moderate impact velocities.

Guo and Gibson [41] analyzed regular hexagonal honeycomb consisting of missing cells using finite element analysis. It was determined that single isolated defects reduce the modulus and strength. The effect of separation distance of the defects was also studied and it was determined that two closely spaced separate defects interact to reduce the elastic buckling strength whereas defects separated by about ten cells act independently.

Li et al [42] studied the elastic properties of two-dimensional voronoi honeycombs with cell shape and cell wall thickness variations. It was determined that for irregular honeycombs with uniform cell wall thickness, the elastic moduli increase considerably with cell shape irregularities while the Poisson's ratios change insignificantly.

Simone and Gibson [17] investigated the effects of plateau borders on the properties of hexagonal honeycomb. It was shown that cell wall material distribution has very little effect on the elastic modulus as the maximum bending occurs at the joints. Simone and

Gibson [43] also studied the effects of cell face curvature and corrugation on the stiffness of regular honeycomb. These results indicated that the modulus and peak stress decrease significantly with the presence of cell face curvature and corrugations and it can be up to 60% of compared to flat faced honeycombs depending upon the relative density.

1.9 Objectives of Present Work

The main objective of this thesis is to study the effects of defects on the performance of regular, first order and second order hierarchical honeycomb cellular structures realized through additive manufacturing process. Specifically, the variation of stiffness would be the focus of this study. The general method used in this study is:

(a) Design and manufacture (through AM process) regular, first order and second order hierarchical honeycomb cellular structures to determine common defects present in FDM processing.

(b) Develop Finite Element Models of the structures using a commercially available tool to study the effective elastic modulus in both axial and transverse directions.

(c) Compare the variations on the performance among all three structure with various percentage of missing cell walls.

(d) Experimentally test the manufactured samples through AM process and compare the experimental outcomes with simulated results.

CHAPTER 2 - METHODOLOGY

2.1 Fabrication using Additive Manufacturing

Samples of regular (zeroth order), first order and second order hierarchical honeycomb were fabricated using fused filament fabrication (FFF) AM process to learn about common manufacturing errors and pitfalls. To adequately understand common manufacturing problems, several common consumer-grade 3D printers with 0.4 mm nozzle diameter were used to create the initial samples and determine what type of defects may be present. Several regular hexagonal honeycomb (ρ = 0.1155, a = 16 mm, t = 1.6mm), first order hierarchical honeycomb (γ_1 = 0.3 and t = 1.2 mm), second order hierarchical honeycomb (γ_2=0.125 and t = 0.8 mm) including the use of different slicing software. ABS (Acrylonitrile Butadiene Styrene) thermoplastic filament was used as the printing material.

It was not geometrically possible to maintain perfect target density for the printed samples due to the resolution limitation of the printers (relative density was between 2% - 2.3% of the target density). A depth of 10 mm was kept for the samples. All structures have 5 cells in Y direction and 3 cells in X direction. Each of the samples had similar manufacturing defects present. Two of the most common defects present were due to errors in extrusion consistency, which resulted in inconsistent walls, and weak joint connections due to the difficulties in developing a perfect toolpath for cellular hexagonal shapes. Depending upon the type of AM process, additively manufactured cellular structures might have several types of microstructural/macrostructural variation or defects. In case of hierarchical honeycomb structures, defects include missing cell walls, partial missing cell walls, disconnected joints, filled cells, irregular thickness etc. Some of the defects might

result in large variations on overall performance, while others have less significant effects on the performance of the structure. To investigate the effects of defects on the structures, randomly missing cell walls were intentionally added into the structure and samples were fabricated for experimental testing. Figure 20 shows additively manufactured samples of intact (without defect) regular, first order and second order hierarchical honeycomb structures. Figure 21 shows representative sample each type of honeycomb with certain percentage of missing cell walls.

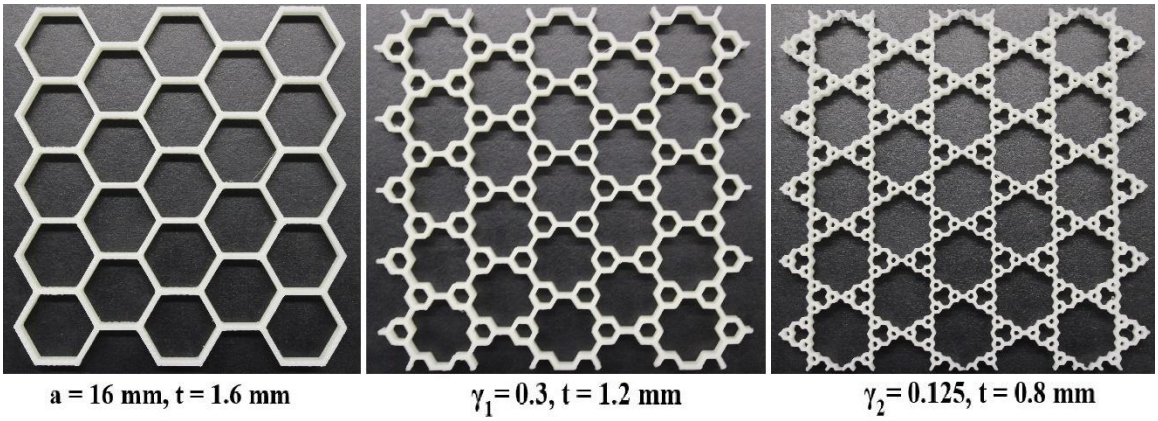

Figure 20: Additively Manufactured samples of (from left to right) regular, first order and second order hierarchical honeycomb

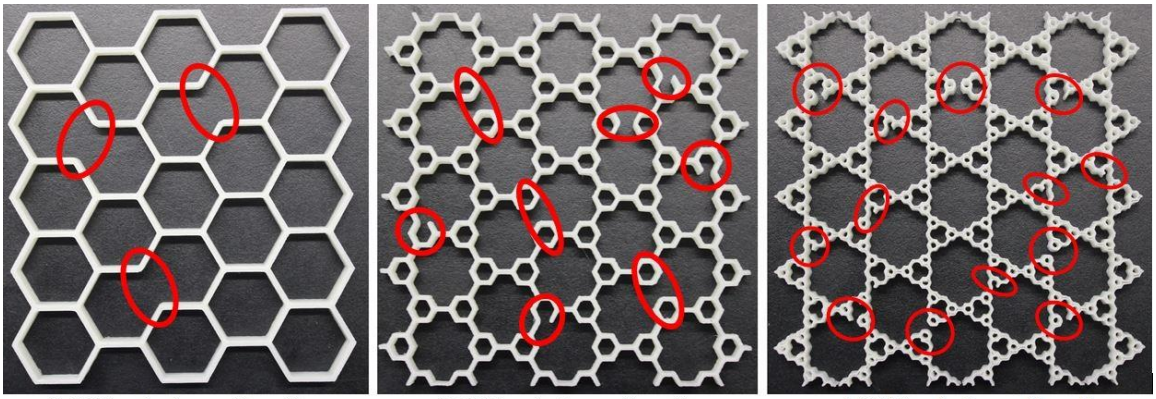

Figure 21: Additively manufactured representative samples of regular, first order and second order hierarchical honeycomb with defects (defect positions circled) by mass density

2.2 Effective Elastic Modulus

The elastic modulus of the structures in both X and Y direction was determined through finite element analysis. The uniaxial compressive response was determined under static loading. The effective elastic modulus of the structures was calculated as:

$$E_{\mathrm{x}} = \frac{F_x}{A_x \varepsilon_x} \tag{21}$$

$$E_{\mathrm{y}} = \frac{F_y}{A_y \varepsilon_y} \tag{22}$$

Where,

E_x = Effective elastic modulus in X direction (transverse)

E_y = Effective elastic modulus in Y direction (axial)

F_x = Calculated compressive load due to the applied displacement in X direction

F_y = Calculated compressive load due to the applied displacement in Y direction

ε_x = Applied compressive strain in X direction

ε_y = Applied compressive strain in Y direction

A_x = Cross-sectional area of the structure in X direction

A_y = Cross-sectional area of the structure in Y direction

2.3 Finite Element Model

Finite element models of additively manufactured exact structures of regular (zeroth order), first order and second order hierarchical honeycomb were prepared using ANSYS® (ANSYS Inc., Cecil Township, PA) parametric design language (APDL). Cell walls of the structures were modeled as 3D eight-node SOLID185 element type with three degrees of freedom at each node. The material was assumed to be isotropic and linearly elastic. Material properties of the isotropic elastic material was taken as the properties of ABS (Acrylonitrile Butadiene Styrene) thermoplastic (Young's modulus, E = 2.4 GPa, Poisson's ratio, $\nu = 0.3$). Initially, all three type of structures were modeled and simulated without any defects to determine baseline elastic behavior to compare to results from structures with defects present. Next, defects were added to the structures in the form missing walls at random locations. Figure 22-27 show the finite element model of regular, first order and second order hierarchical honeycomb and zoomed in section of the finite element mesh of all three.

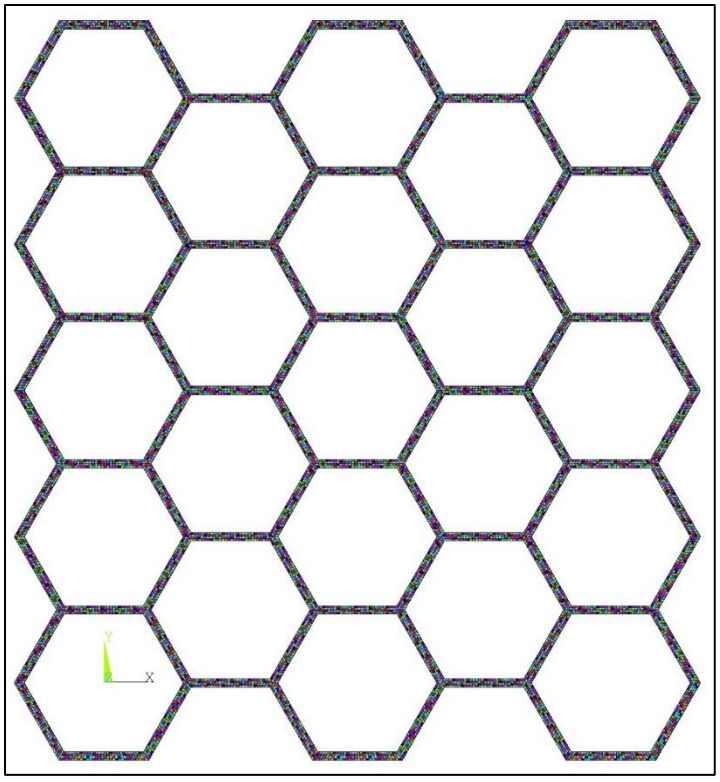

Figure 22: Finite element model of regular honeycomb structure. Number of Elements = 178848

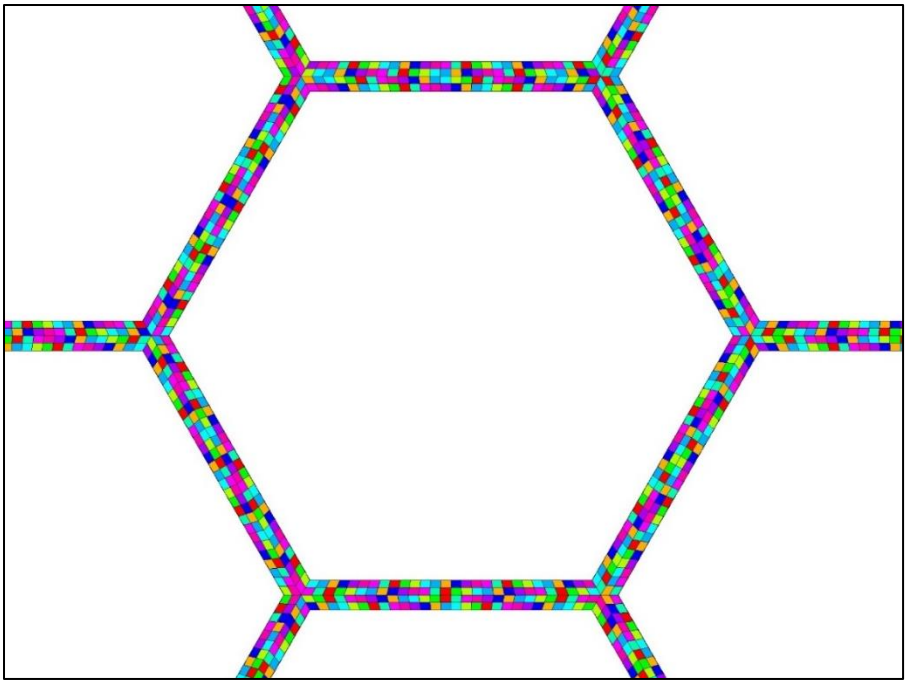

Figure 23: Finite element mesh of regular honeycomb (zoomed in)

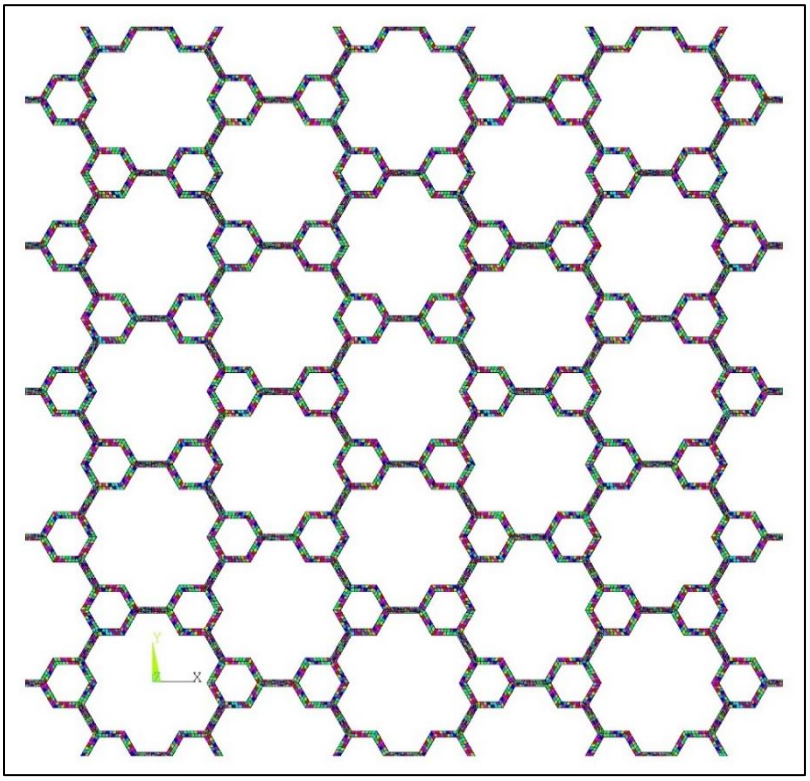

Figure 24: Finite element model of first order hierarchical honeycomb. Number of elements = 127680

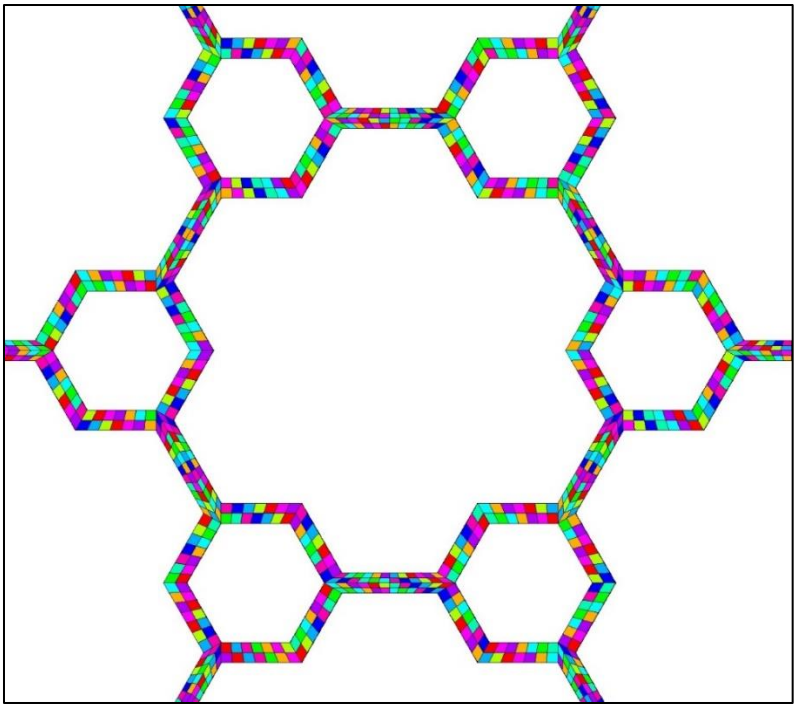

Figure 25: Finite element mesh of first order hierarchical honeycomb (zoomed in)

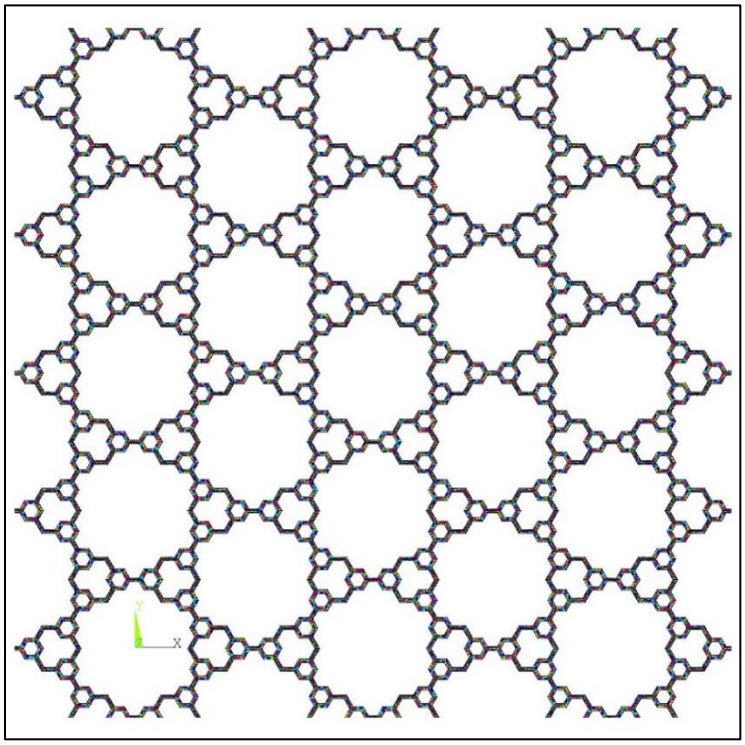

Figure 26: Finite element model of second order hierarchical honeycomb. Number of elements = 163536

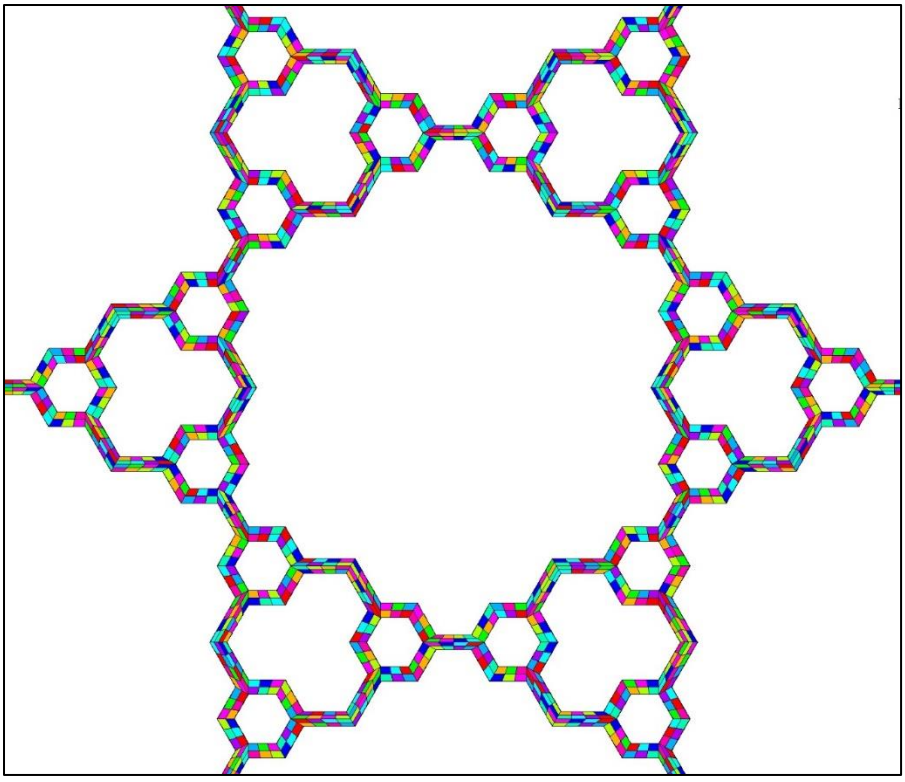

Figure 27: Finite element mesh of second order hierarchical honeycomb (zoomed in)

To calculate the stiffness in axial direction (Y direction), a compressive displacement was applied at the extreme top nodes in negative Y direction. The bottom surface of the model was fixed to eliminate displacement in the X and Y directions. The model was also fixed at halfway through the Z direction depth to eliminate any Z direction movement and/or rotation. To consider symmetry, the X direction movements were constrained at all the extreme left nodes. Figure 28A shows the boundary conditions in regular honeycomb structure (Z direction constraint is not shown for clear view). Figure 28B shows the right view with Z direction constraint included.

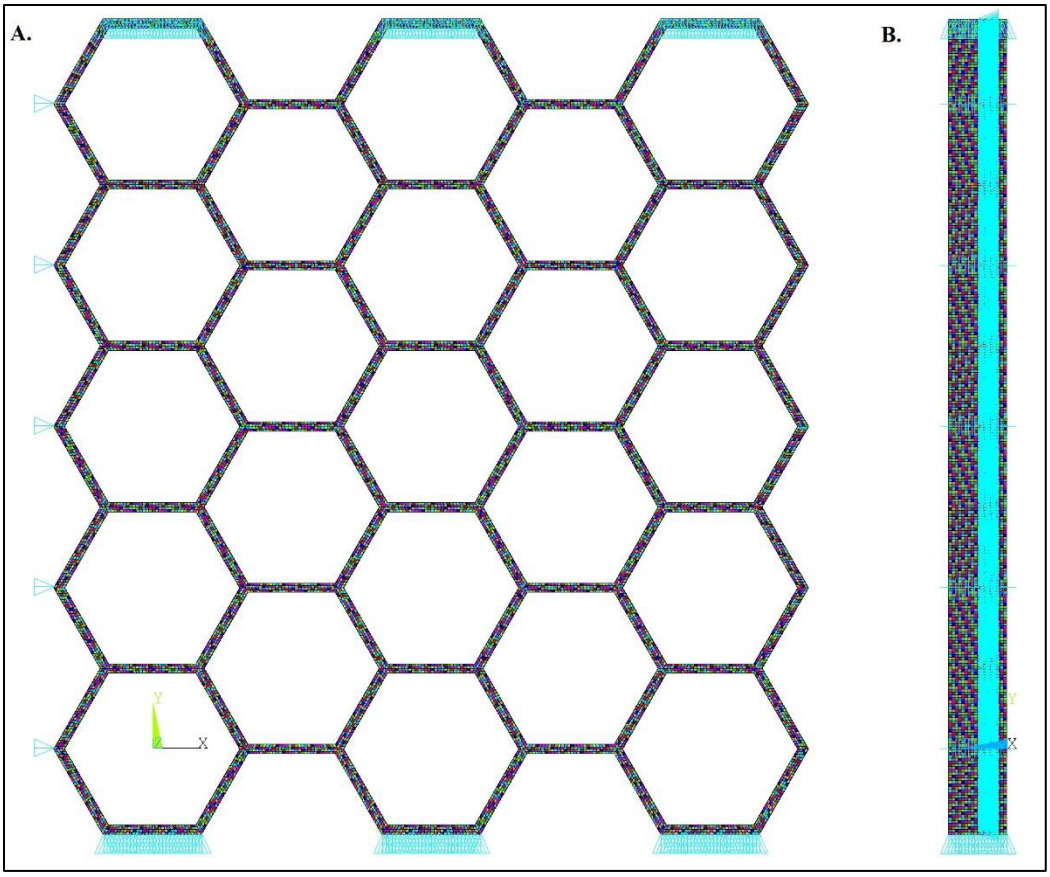

Figure 28: Regular honeycomb boundary conditions axial stiffness **A.** boundary conditions without Z direction constraint. **B.** right view of boundary conditions with Z direction constraint

To calculate the transverse stiffness (X direction), the same boundary conditions were applied with the only exception of the compressive displacement in X direction. The displacement boundary condition was applied to the extreme X nodes at the right edge of the model. The boundary conditions can be seen in Figure 29.

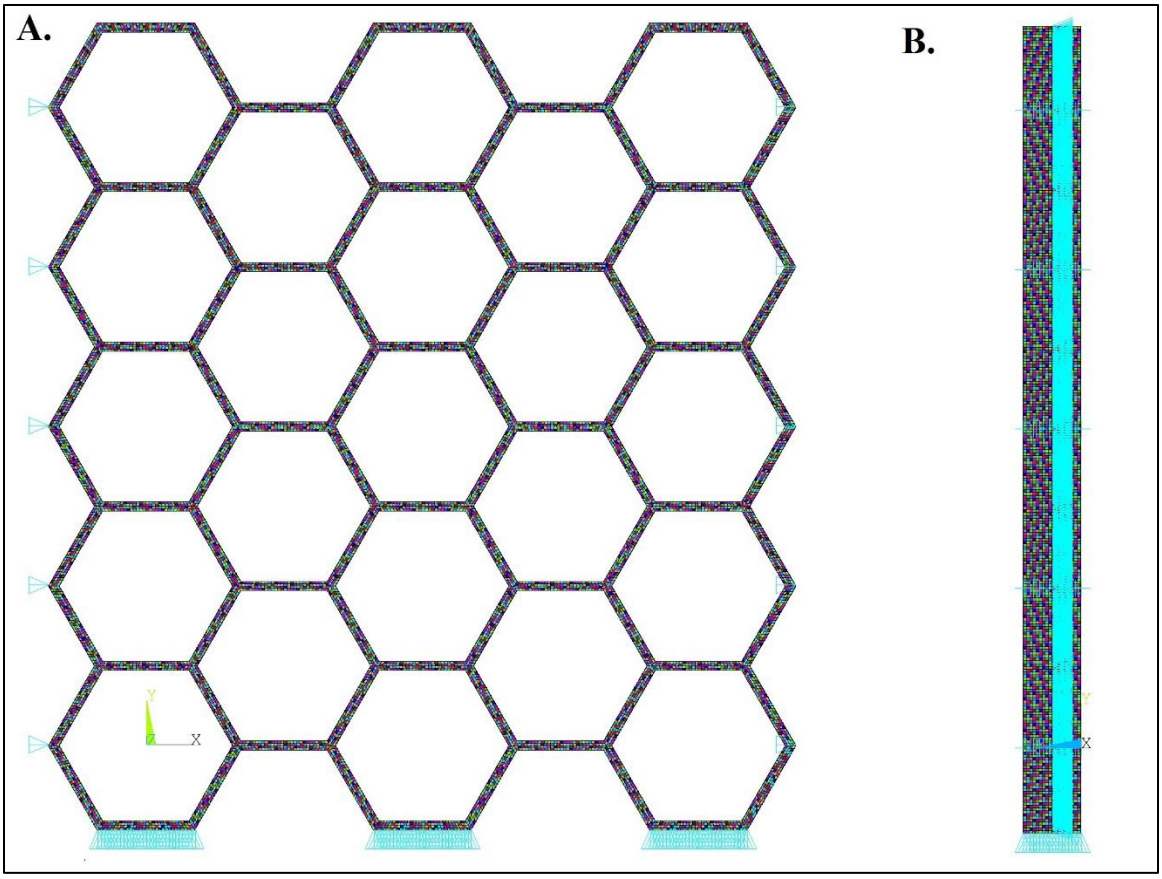

Figure 29: Regular honeycomb boundary conditions for transverse stiffness A. boundary conditions without Z direction constraint. B. right view of boundary conditions with Z direction constraint

2.4 Experimental Methods

To compare the simulation results with experimental results, uniaxial in-plane compressive testing was performed using MTS Insight 5 universal testing machine (see Figure 30 for the experimental setup). The machine uses a 5kN load cell to measure force, which is later converted to stress, and a built in LVDT (linear variable differential transformer) to measure displacement, which was later converted to strain. The compressive stress-strain data are utilized to calculate the elastic modulus of the structures. Two parallel plates were used to compress the samples.

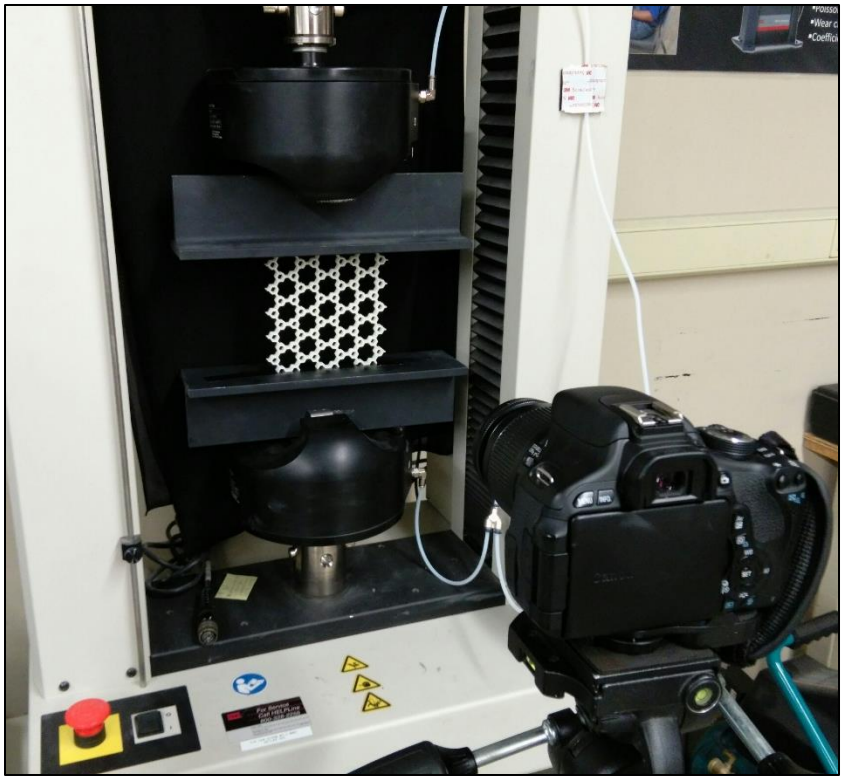

Figure 30: Experimental setup for uniaxial compressive testing

CHAPTER 3 - RESULTS AND DISCUSSIONS

3.1 Introduction

The elastic modulus of non-defective structures in the X and Y direction were first determined. These elastic modulus results were utilized to normalize the elastic modulus of the cellular structures with incorporated defects. The normalized elastic modulus in both axial and transverse directions have been plotted as a function of the percentage of defects by mass density to understand the effect of defects on the stiffness. Additively manufactured samples of all three types of hierarchical honeycomb structures containing different percentage of defects in the form of random missing cell walls have been tested to determine the experimental elastic modulus of those structures. The experimental data have been analyzed using a MATLAB® (The MathWorks Inc., Natick,MA) code (see APPENDIX D) to determine the elastic modulus of the structures. The elastic modulus has been calculated from the stress-strain curve of the individual structure. Figure 31 shows a representative stress-strain curve of regular honeycomb.

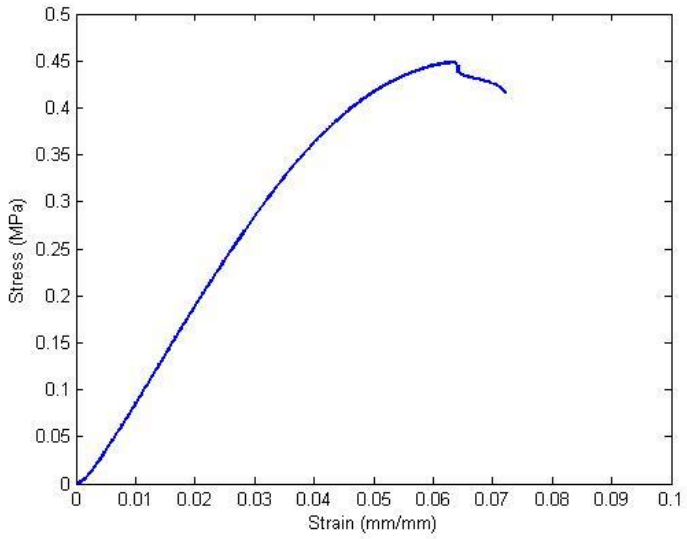

Figure 31: A typical stress-strain curve of a regular honeycomb structure.

3.2 Effect of defects on Stiffness

ANSYS simulations were used to determine the elastic modulus of the regular, first order and second order hierarchical honeycomb in axial direction (Table 1) and transverse direction (Table 2).

Table 1: Elastic Modulus of regular, first order and second order hierarchical honeycomb in axial direction from FEA simulations

Honeycomb Type	Cross-sectional Area, A (mm^2)	Compressive Load, F (N)	Compressive Stress ,σ (MPa)	Compressive Strain, ε (mm/mm)	Elastic Modulus, E (MPa)
Regular Honeycomb	1298.5	268.58	0.2068	0.03	6.89
First order Hierarchy	1440	999.09	0.6938	0.03	23.13
Second order Hierarchy	1440	2835.50	1.9691	0.03	39.38

Table 2: Elastic Modulus of regular, first order and second order hierarchical honeycomb in transverse direction from FEA simulations

Honeycomb Type	Cross-sectional Area, A (mm_2)	Compressive Load, F (N)	Compressive Stress ,σ (MPa)	Compressive Strain, ε (mm/mm)	Elastic Modulus, E (MPa)
Regular Honeycomb	1401.6	220.80	0.1575	0.03	5.25
First order Hierarchy	1385.6	1380.18	0.9961	0.03	19.92
Second order Hierarchy	1385.6	2201.30	1.5887	0.03	31.77

3.2.1 Regular honeycomb structure stiffness

(a) Axial Stiffness

Two different approaches were used to study the defects in regular hexagonal honeycomb. First, consideration was given to the orientation of the defect(s) and the effects on the elastic modulus of the structure. Random sets of horizontal or inclined cell walls were removed and the normalized elastic modulus was determined from the simulation. For this type of analysis, either only horizontal walls were randomly selected or only inclined walls were randomly selected to be removed. From this analysis, it was determined that missing inclined cell walls significantly decrease the elastic modulus compared to missing horizontal cell walls (see Figure 32).

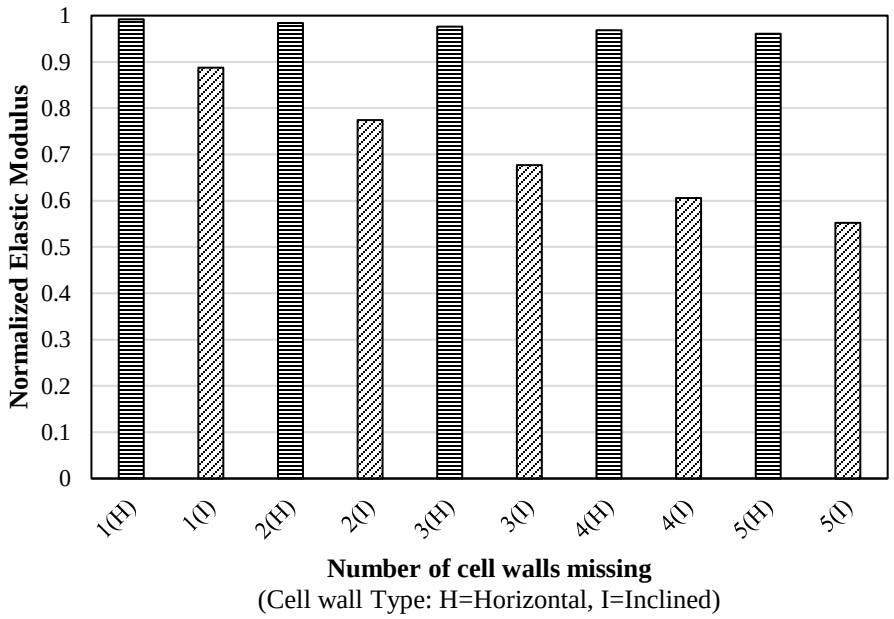

Figure 32: Effect of orientation of missing cell walls on the elastic modulus of regular honeycomb

Next, four sets of defects, regardless of defect orientation, were randomly chosen. This included a combination of horizontal and inclined defects in each set (see Figure 33 for example of defects). Figure 34 shows a sample of deformation of the structure with defects in X direction under axial compressive loading.

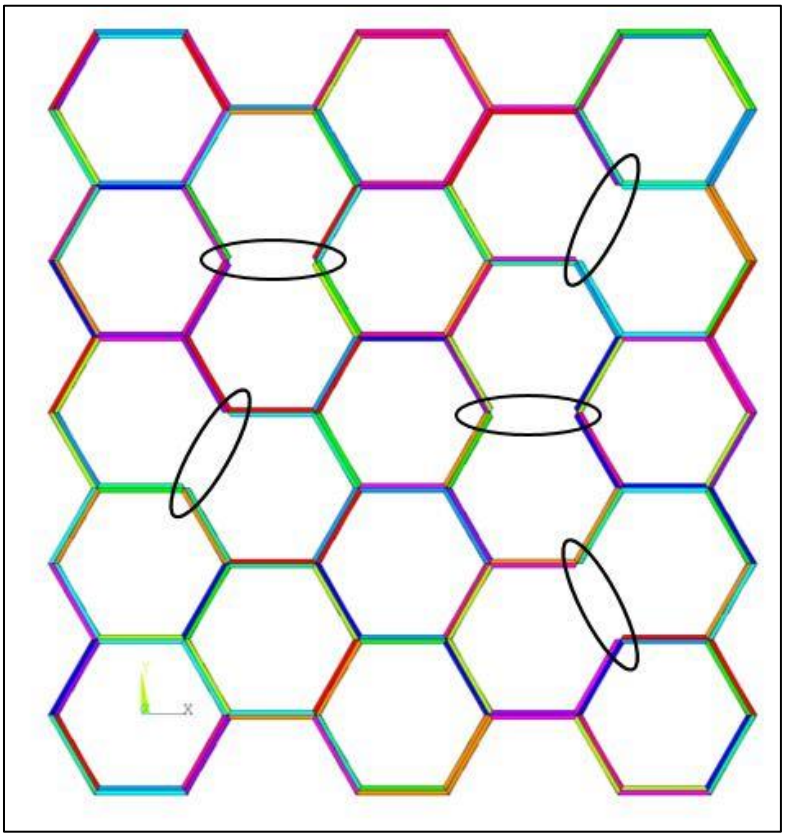

Figure 33: Examples of horizontal and inclined defects in regular honeycomb

As shown in Figure 35, the deviation of elastic modulus for each set of data is large depending on the types of defects randomly chosen. Simulations that include more inclined defects tend to have lower overall elastic modulus values. Also, as the percentage of defects increase, the deviation range of results also increases. On average, the elastic modulus decreased by about 45% at about 5.5% randomly missing cell walls by mass.

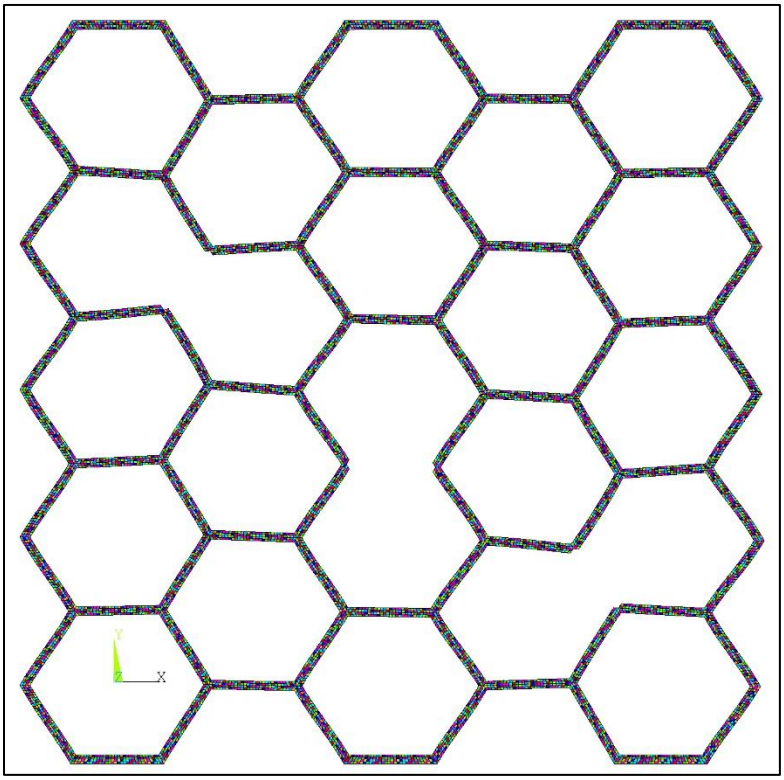

Figure 34: Response of regular honeycomb under axial compressive loading

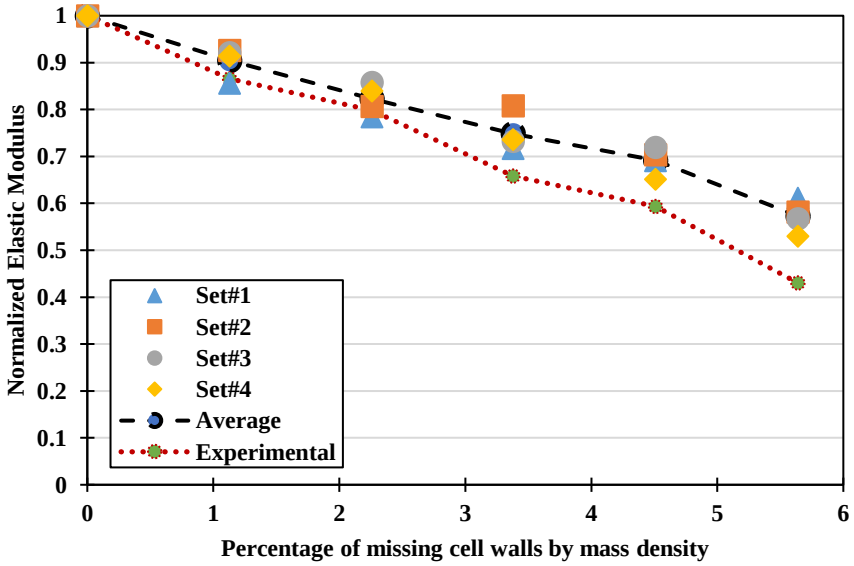

Figure 35: Effect of missing cell walls on the elastic modulus of regular honeycomb in axial direction

(b) Transverse Stiffness

The same four sets of defects were chosen to determine the transverse stiffness behavior of the structures with defects. Figure 36 shows a sample of the deformation of the structure with defects in Y direction under transverse compressive loading. As shown in Figure 37, the reduction in the elastic modulus of regular honeycomb with defects in transverse direction is very similar to that in the axial direction. On average, the elastic modulus decreased by about 45% at about 5.5% randomly missing cell walls by mass.

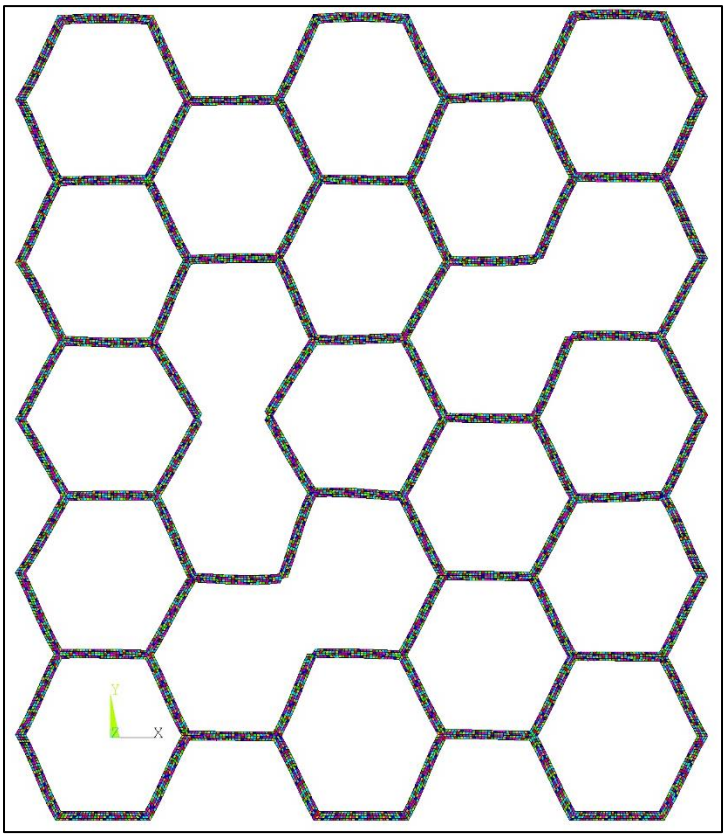

Figure 36: Response of regular honeycomb under transverse compressive loading.

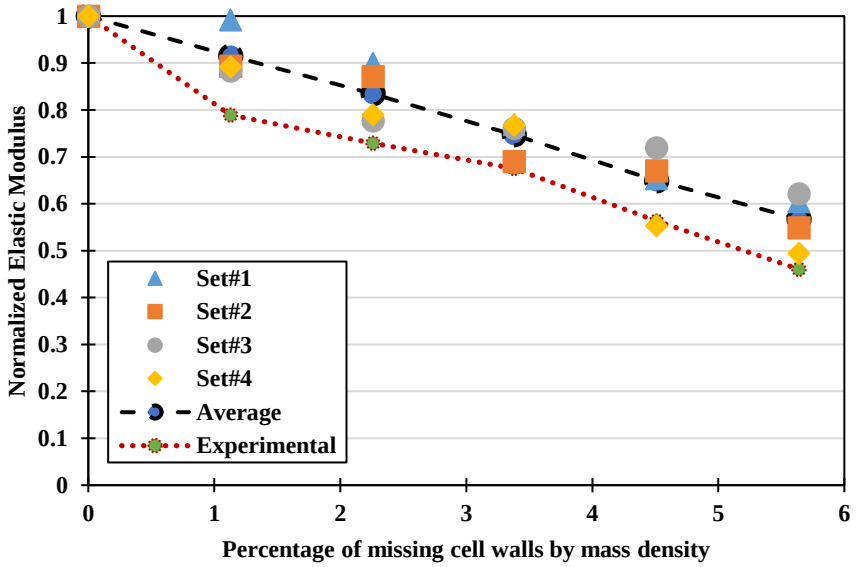

Figure 37: Effect of missing cell walls on the elastic modulus of regular honeycomb in transverse direction

3.2.2 First order hierarchical honeycomb stiffness

(a) Axial Stiffness

To investigate the effect of missing cell walls on the first order hierarchical honeycomb, randomly selected cell walls were removed without regard to whether the cell wall was horizontal/inclined or from the regular honeycomb structure or the first order honeycomb structure. Figure 38 shows a representative finite element model of first order hierarchy with missing cell walls. Four sets or randomly chosen defects were simulated to determine the elastic modulus with the presence of defects. Figure 40 shows the normalized elastic modulus of the first order hierarchical honeycomb as a function of missing cell walls percentage. The results of these simulations show, on average, the elastic modulus is reduced by more than 60% for approximately 4% missing cell walls by mass. Experimental results, although showing a very similar normalized trend, are actually higher. This is likely due to the "non-defective" sample used to normalize the defective results actually have

some manufacturing problems leading to lower stiffness. Overall, the effect of defects was much stronger for first order hierarchy than the zero order (regular honeycomb).

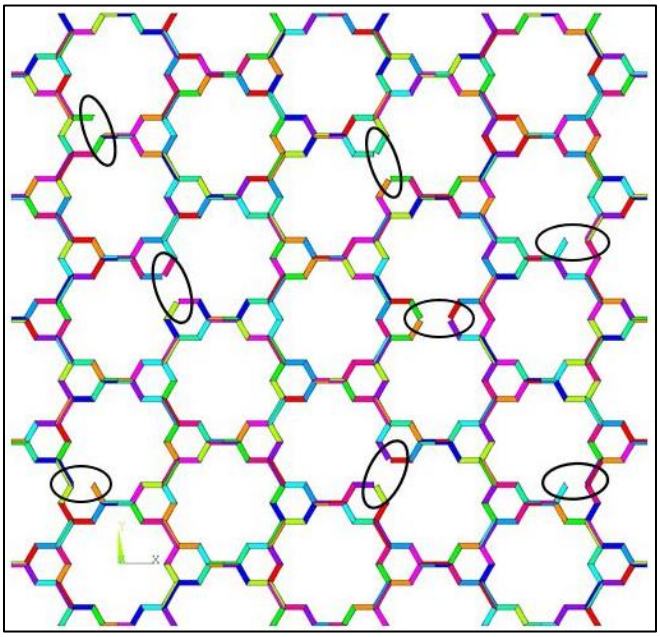

Figure 38: Examples of defects in first order hierarchical honeycomb

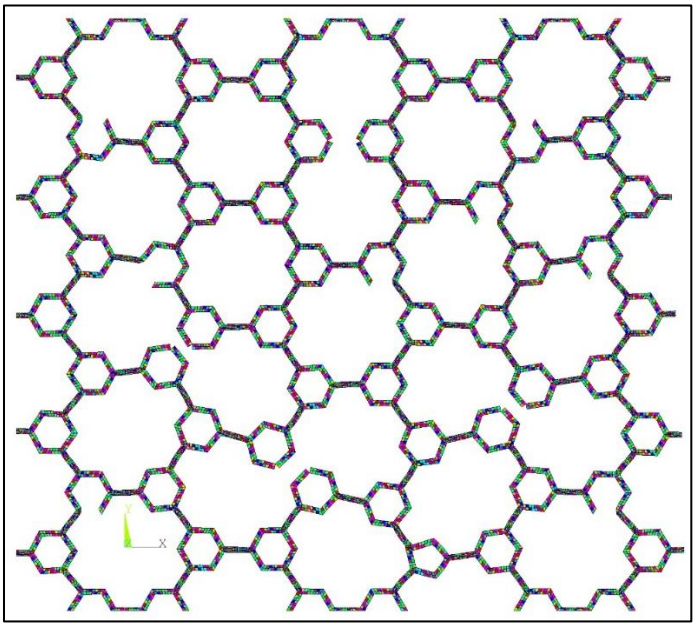

Figure 39: Response of first order hierarchical honeycomb with defects under axial loading

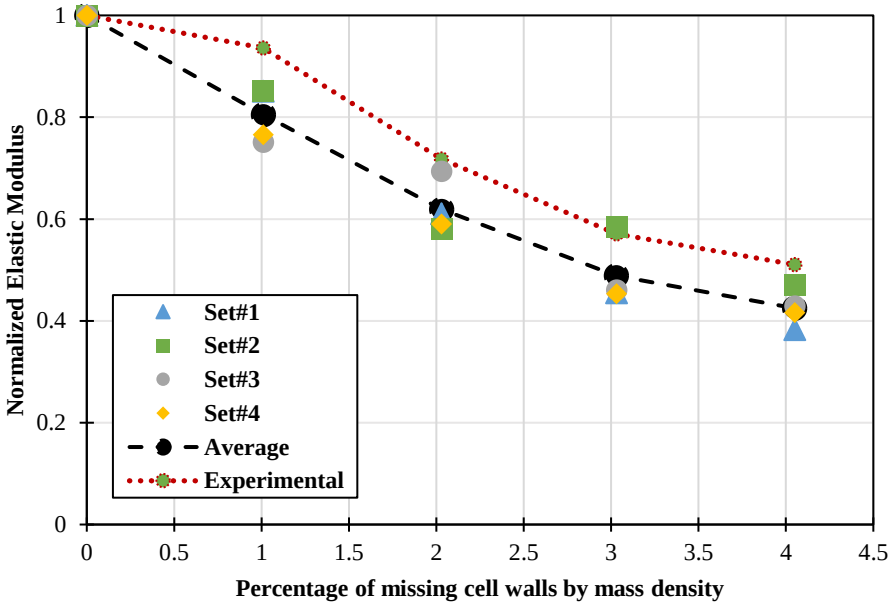

Figure 40: Effect of missing cell walls on first order hierarchical honeycomb structure under axial loading

(b) Transverse Stiffness

To determine the effect of missing cell walls on the transverse stiffness, the same types of random defects were chosen as in the case of axial stiffness of first order hierarchical honeycomb. Figure 41 shows a representative sample with deformation of first order hierarchical honeycomb under transverse compressive loading. Simulations show, on average, the elastic modulus decreased by about 70% with more than 4% missing cell walls (as shown in Figure 42). Experimental results show good agreement with simulations when the percentage of defects are low. The elastic modulus decreased by about 80% with more than 4% missing cell walls. Randomness of the missing cell walls and number of experimental results could possibly be the reason of this deviation in experimental results.

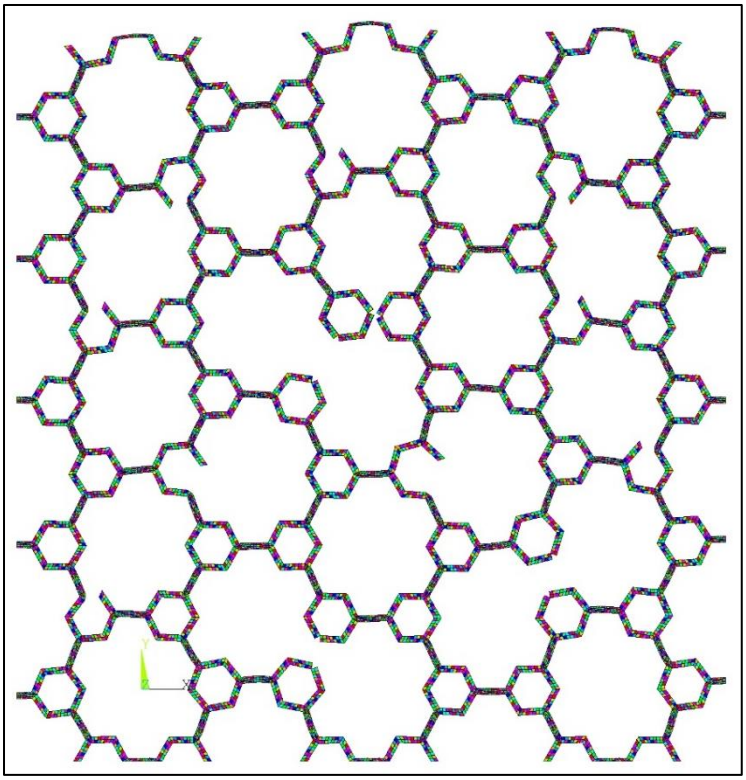

Figure 41: Response of first order hierarchical honeycomb with defects under transverse loading

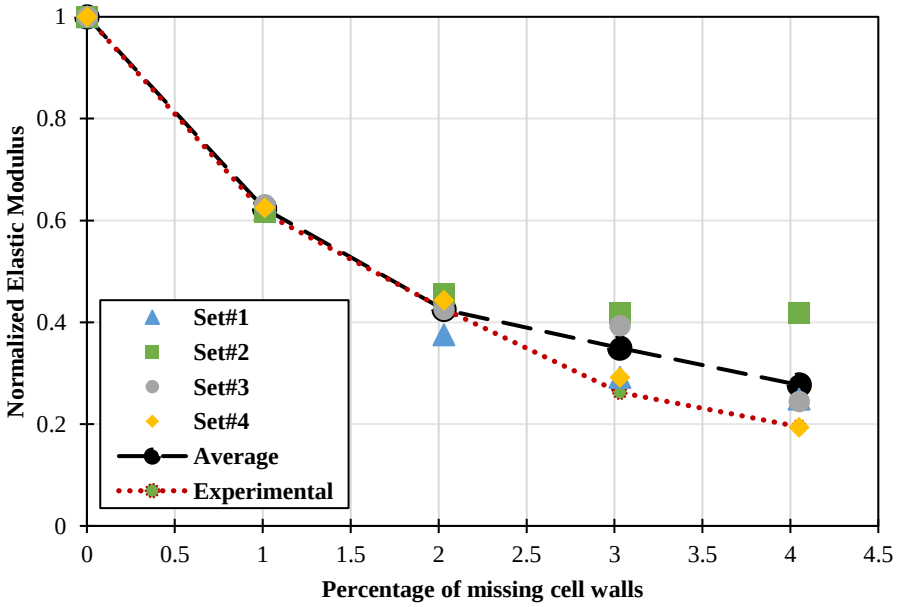

Figure 42: Effect of missing cell walls on the transverse stiffness of first order hierarchical honeycomb structure

3.2.3 Second order hierarchical honeycomb stiffness

(a) Axial Stiffness

Similar to the analysis conducted for first order hierarchical honeycomb structures, the effect of randomly missing cell walls on the elastic properties of second order hierarchical honeycomb structures was investigated by incorporating random defects into the structure without regard for the type of cell wall (horizontal/inclined or regular, first order, or second order). Figure 43 shows the finite element model of a typical second order hierarchical honeycomb with missing cell walls.

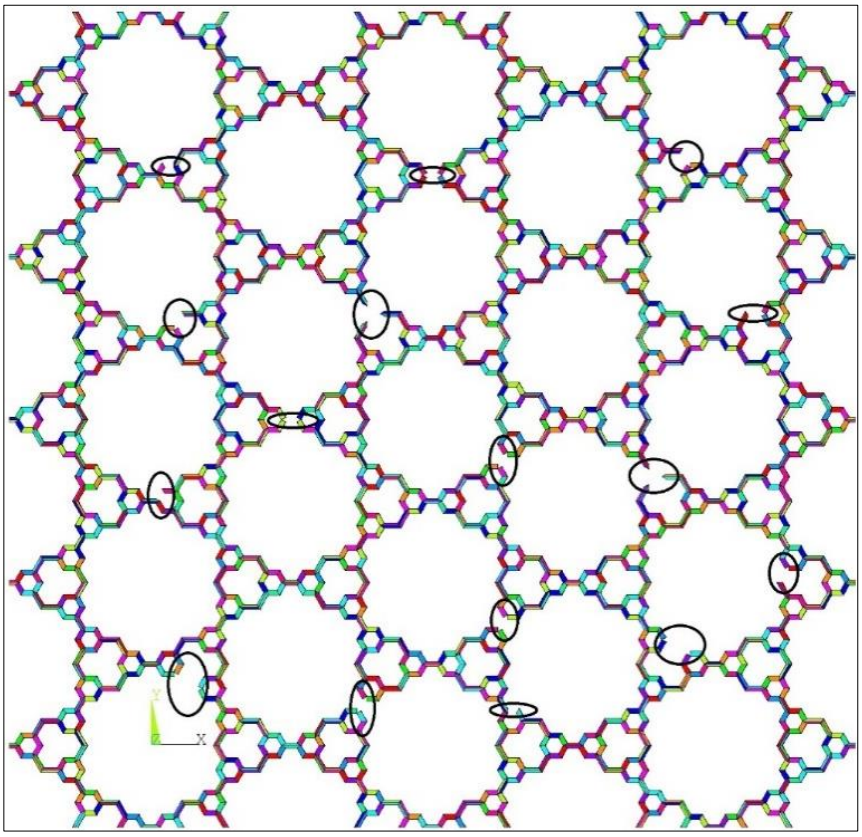

Figure 43: Examples of defects in second order hierarchical honeycomb

Figure 44 shows the normalized elastic modulus for different percentage of missing cell walls. These results indicate that the elastic modulus is decreasing on average, by more than 50% with only 2% missing cell walls by mass. Increasing the number of defects to approximately 4% missing cell walls decreases the elastic modulus by nearly 95%, showing significant differences to both the first order honeycomb and the regular honeycomb. Our experimental results show reasonable agreement with the simulation results.

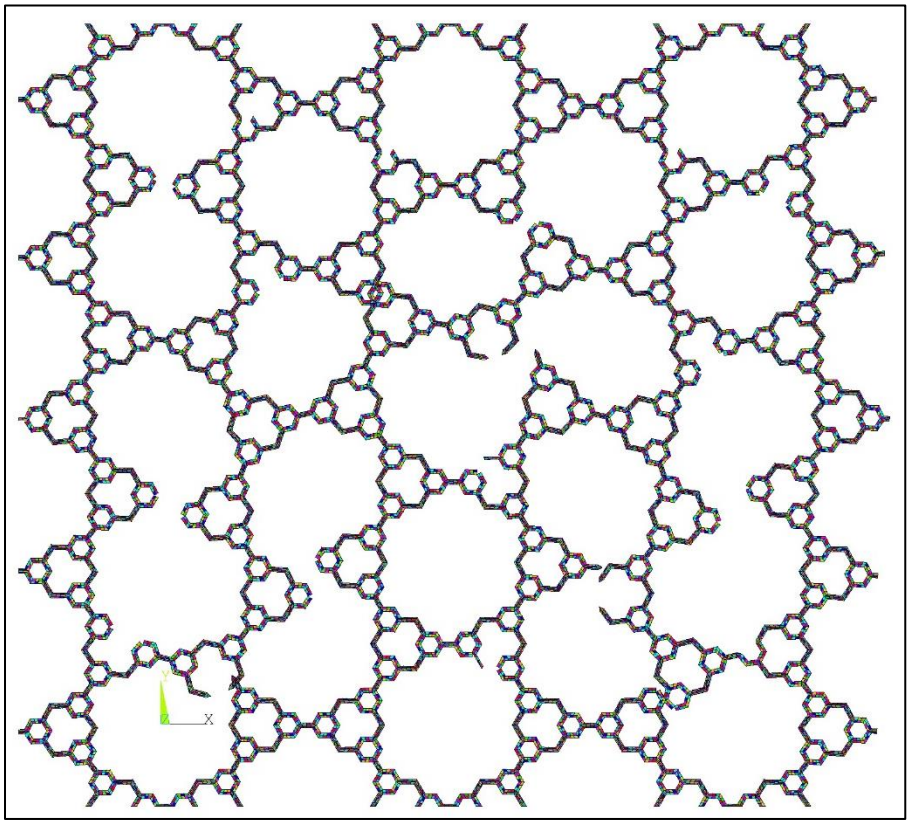

Figure 44: Response of second order hierarchical honeycomb with defects under axial loading

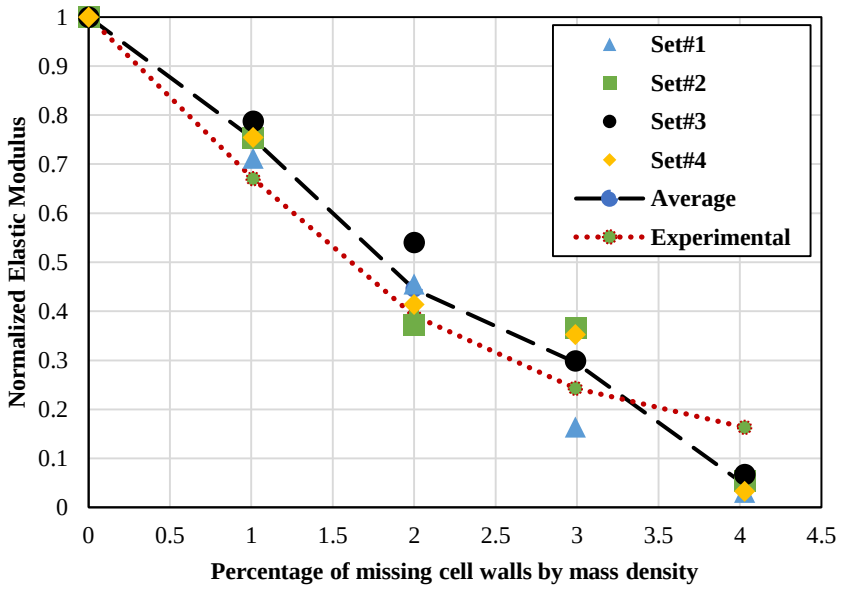

Figure 45: Effect of missing cell walls on the axial stiffness of second order hierarchical honeycomb structure

(b) Transverse Stiffness

To determine the effect of missing cell walls on the transverse stiffness of second order hierarchical honeycomb, similar types of defects were chosen as in the axial stiffness calculations. Figure 46 shows a representative sample of deformation of second order hierarchical honeycomb under transverse compressive loading. Figure 47 shows the normalized elastic modulus as a function of missing cell walls. Simulations show, on average, the elastic modulus decreased by about 95% with more than 4% missing cell walls. Experimental results are in quite good agreement with the simulations.

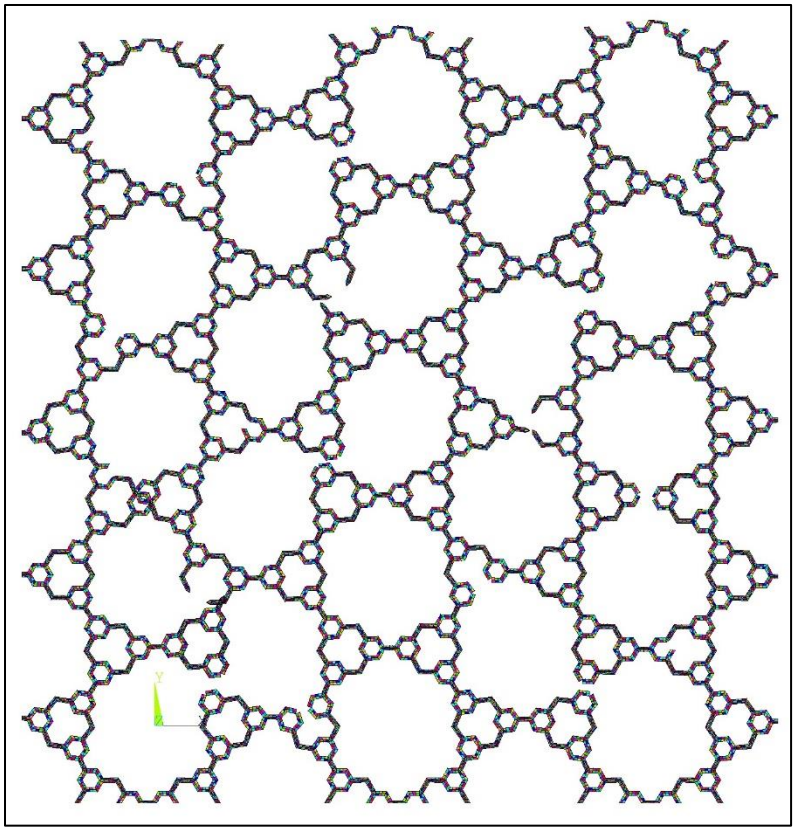

Figure 46: Response of second order hierarchical honeycomb with defects under transverse loading

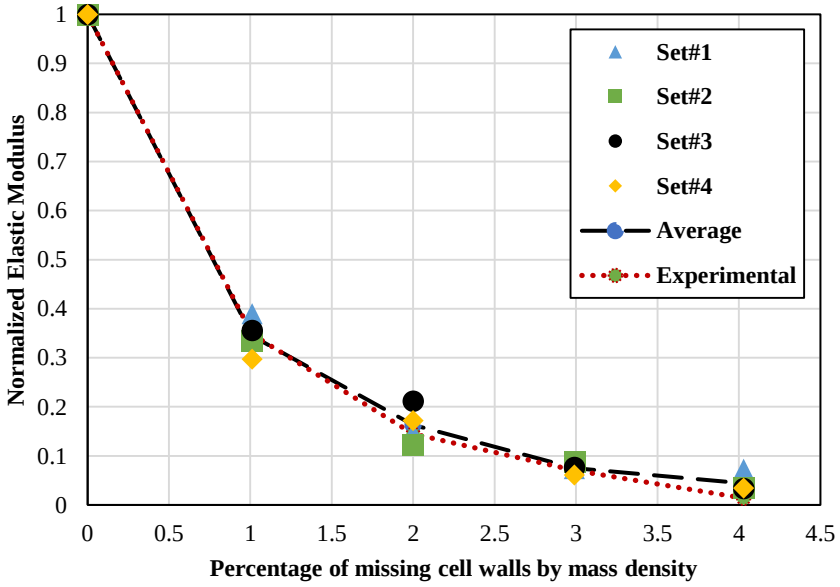

Figure 47: Effect of missing cell walls on the transverse stiffness of second order hierarchical honeycomb structure

CHAPTER 4 - CONCLUSION AND FUTURE WORK

4.1 Conclusions

Cellular metamaterials with hierarchical organization can lead to enhanced mechanical performance without increasing the structural weight. Lightweight yet stiff metamaterials like hierarchical honeycomb structures have complex structure matrix making them very difficult, expensive and wasteful to manufacture using traditional manufacturing technologies. Additive manufacturing technology has eliminated this boundary and is revolutionizing manufacturing across many industries. Extensive hardware and software development is being researched to increase precision in manufacturing, however, additive manufacturing is currently prone to manufacturing variations (defects) such as missing/broken cell walls, irregular thickness, flawed joints, missing (partial) layers, and irregular elastic plastic behavior due to toolpath etc.

In current work, the in-plane stiffness of regular hexagonal, first order and second order hierarchical honeycomb metamaterials have been studied when additive manufacturing defects in the form of missing cell walls are present. Finite element analysis have been carried out using ANSYS®. Additively manufactured samples of the structures have been tested to experimentally verify the simulation results.

Initially, a finite element model of each type of honeycomb without defects was developed to learn the baseline elastic modulus. Defects of different percentages by mass density in the form of missing cell walls have been added intentionally to determine the effects on the elastic modulus of the structures. In plane compressive load with proper boundary conditions was applied to determine the axial and transverse stiffness behavior. From the simulation results, it is concluded that the defects in the form of missing cell walls

has more deleterious effect as the hierarchical order increases (see Figures 48 and 49). On average, the elastic modulus in the axial direction decreased by 45% with 5.5% missing cell walls for regular honeycombs, 60% with 4% missing cell walls for first order hierarchical honeycomb and 95% with 4% missing cell walls for second order hierarchical honeycombs. In the other direction, the transverse elastic modulus decreased by about 45% with more than 5.5% missing cell walls for regular honeycomb, about 75% with 4% missing cell walls for first order and more than 95% with 4% missing cell walls for second order hierarchical honeycomb.

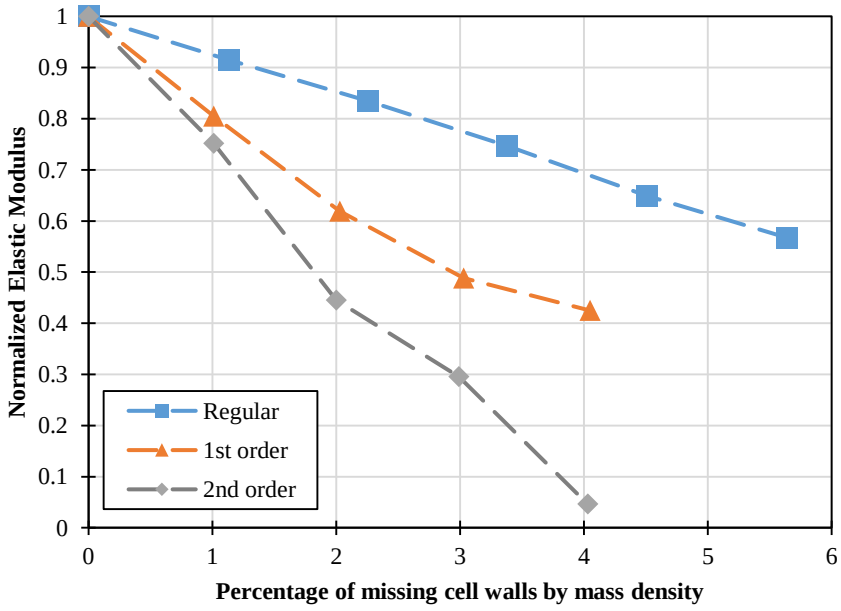

Figure 48: Comparison of axial elastic modulus of hierarchical honeycomb with missing cell walls

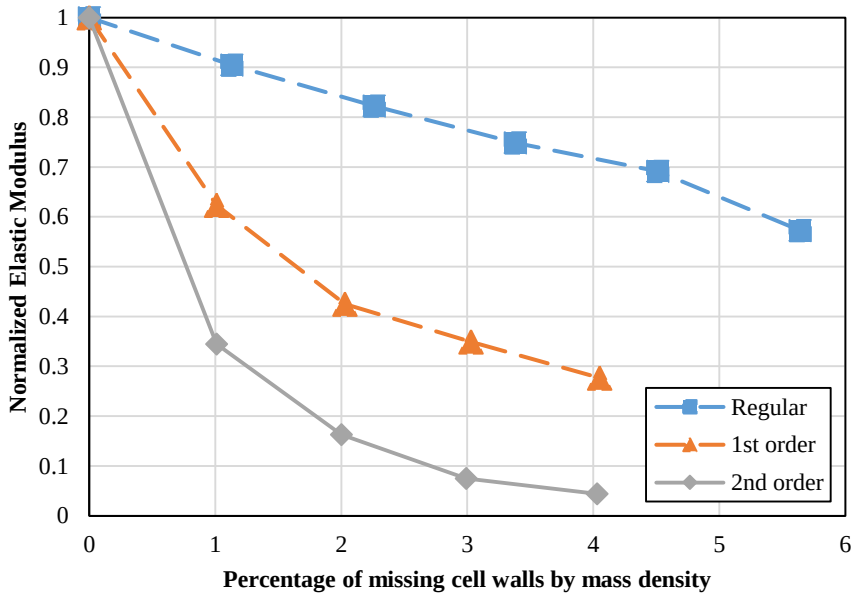

Figure 49: Comparison of transverse elastic modulus of hierarchical honeycomb with missing cell walls

4.2 Future Works

The current study was limited to the stiffness behavior of the honeycomb metamaterials with defects in the form of missing cell walls. Additively manufactured cellular structures can have other types of defects such as filled cells, irregular thicknesses, flawed joints, warped surfaces etc. These defects can possibly affect the performance of the structures significantly and should be studied for a more complete understanding.

In this study, only axial and transverse elastic modulus have been determined for the elastic behavior. Investigating the uniaxial elastic buckling behavior and the plastic behavior of the structures with defects should be considered in future works. Increasing the levels/orders of hierarchy, using different relative density of the structures can also be included in future studies.

The material used in the simulations of this study has been considered linearly elastic and isotropic. In additive manufacturing, the raster orientation, layers thickness etc. can cause variation in the properties and might not show isotropic behavior. Future studies may need to consider non-isotropic modeling to simulations closer to experimental results.

REFERENCES

[1] Gibson, L. J., & Ashby, M. F. (1999). *Cellular solids: structure and properties*. Cambridge university press

[2] Open cell foam; Retrieved from: https://upload.wikimedia.org/wikipedia/commons/8/88/Foam_Open_Cell.jpg

[3] Cancellous bone. (2016). In *Encyclopædia Britannica*. Retrieved from http://www.britannica.com/science/cancellous-bone

[4] Honeycomb, Retrieved from: http://unisci24.com/251936.html

[5] Microstructure Materials (2009). Retrieved from http://smartmaterials2009.blogspot.com/2009/09/wood_14.html

[6] Types of spray foam insulation. (2013).in Spray Foam Insulation Phoenix, AZ. Retrieved from: http://sprayfoaminsulationphoenix.net/types-of-spray-foam-insulation

[7] Ajdari, A., Jahromi, B. H., Papadopoulos, J., Nayeb-Hashemi, H., & Vaziri, A. (2012). Hierarchical honeycombs with tailorable properties. *International Journal of Solids and Structures*, *49*(11), 1413-1419

[8] Zhang, Z., Zhang, Y. W., & Gao, H. (2011). On optimal hierarchy of load-bearing biological materials. *Proceedings of the Royal Society of London B: Biological Sciences*, *278*(1705), 519-525.

[9] Rayneau-Kirkhope, D., Mao, Y., & Farr, R. (2012). Ultralight fractal structures from hollow tubes. *Physical review letters*, *109*(20), 204301.

[10] Mousanezhad, D., Babaee, S., Ebrahimi, H., Ghosh, R., Hamouda, A. S., Bertoldi, K., & Vaziri, A. (2015). Hierarchical honeycomb auxetic metamaterials. *Scientific reports*, *5*.

[11] Mousanezhad, D., Ebrahimi, H., Haghpanah, B., Ghosh, R., Ajdari, A., Hamouda, A. M. S., & Vaziri, A. (2015). Spiderweb honeycombs. *International Journal of Solids and Structures*, *66*, 218-227.

[12] Fan, H. L., Jin, F. N., & Fang, D. N. (2008). Mechanical properties of hierarchical cellular materials. Part I: Analysis. *Composites Science and Technology*, *68*(15), 3380-3387.

[13] Kooistra, G. W., Deshpande, V., & Wadley, H. N. (2007). Hierarchical corrugated core sandwich panel concepts. *Journal of applied mechanics*, *74*(2), 259-268.

[14] Taylor, C. M., Smith, C. W., Miller, W., & Evans, K. E. (2011). The effects of hierarchy on the in-plane elastic properties of honeycombs. *International Journal of Solids and Structures*, 48(9), 1330-1339.

[15] Lukkassen, D. (1997). Bounds and homogenization of optimal reiterated honeycombs. *Computer Aided Optimum Design of Structures V, Computational Mechanics Publications, Southhampton*, 267-276.

[16] Oftadeh, R., Haghpanah, B., Vella, D., Boudaoud, A., & Vaziri, A. (2014). Optimal fractal-like hierarchical honeycombs. *Physical review letters*, *113*(10), 104301.

[17] Simone, A. E., and L. J. Gibson. "Effects of solid distribution on the stiffness and strength of metallic foams." Acta Materialia 46.6 (1998): 2139-2150.

[18] Lyons, B. (2014). Additive manufacturing in aerospace: examples and research outlook. *The Bridge*, *44*(3).

[19] Giffi, C., Gangula, B., & Illinda, P. (2014). 3D opportunity for the automotive industry: Additive manufacturing hits the road.

[20] Murr, L. E., Gaytan, S. M., Medina, F., Lopez, H., Martinez, E., Machado, B. I., ... & Bracke, J. (2010). Next-generation biomedical implants using additive manufacturing of complex, cellular and functional mesh arrays. *Philosophical Transactions of the Royal Society of London A: Mathematical, Physical and Engineering Sciences*, *368*(1917), 1999-2032.

[21] Camisa, J. A., Verma, V., Marler, D. O., & Madlinger, A. (2014, August 7). Additive Manufacturing and 3D Printing for Oil and Gas - Transformative Potential and Technology Constraints. International Society of Offshore and Polar Engineers.

[22] Ning, F., Cong, W., Qiu, J., Wei, J., & Wang, S. (2015). Additive manufacturing of carbon fiber reinforced thermoplastic composites using fused deposition modeling. *Composites Part B: Engineering*, *80*, 369-378.

[23] Cerneels, J., Voet, A., Ivens, J., & Kruth, J. P. (2013, September). Additive manufacturing of thermoplastic composites. In *Composites Week@ Leuven* (pp. 1-7). KU Leuven.

[24] Scheithauer, U., Schwarzer, E., Richter, H. J., & Moritz, T. (2015). Thermoplastic 3D Printing—An Additive Manufacturing Method for Producing Dense Ceramics. *International Journal of Applied Ceramic Technology*, *12*(1), 26-31.

[25] Frazier, W. E. (2014). Metal additive manufacturing: a review. *Journal of Materials Engineering and Performance*, *23*(6), 1917-1928.

[26] Bose, S., Vahabzadeh, S., Ke, D., & Bandyopadhyay, A. (2015). Additive Manufacturing of Ceramics. *Additive Manufacturing*, 143.

[27] Luo, J., Pan, H., & Kinzel, E. C. (2014). Additive Manufacturing of Glass. *Journal of Manufacturing Science and Engineering*, *136*(6), 061024.

[28] P.F. Jacobs, Rapid prototyping and Manufacturing: Fundamentals of Stereolithography, pp 11-18, Society of Manufacturing Engineers, Dearborn, MI,1992

[29] Griffith, M. L., & Halloran, J. W. (1996). Freeform fabrication of ceramics via stereolithography. *Journal of the American Ceramic Society*, *79*(10), 2601-2608.

[30] Powder Bed AM, Lawrence Livermore National Laboratory. Retrieved from: https://acamm.llnl.gov/am-technology/powder-bed-am

[31] Wong, K. V., & Hernandez, A. (2012). A review of additive manufacturing. *ISRN Mechanical Engineering*, *2012*.

[32] EBM Hardware, retrieved from: http://www.arcam.com/technology/electron-beam-melting/hardware/

[33] Taminger, K. M., & Hafley, R. A. (2006). Electron beam freeform fabrication for cost effective near-net shape manufacturing.

[34] 3D printing, Retrieved from: http://www.custompartnet.com/wu/3d-printing

[35] Material Jetting, Retrieved from: http://www.me.vt.edu/dreams/material-jetting

[35] Prakash, O., Bichebois, P., Brechet, Y., Louchet, F., & Embury, J. D. (1996). A note on the deformation behaviour of two-dimensional model cellular structures. *Philosophical Magazine A*, *73*(3), 739-751.

[36] Ajdari, A., Nayeb-Hashemi, H., Canavan, P., & Warner, G. (2008). Effect of defects on elastic–plastic behavior of cellular materials. *Materials Science and Engineering: A*, *487*(1), 558-567.

[37] Silva, M. J., & Gibson, L. J. (1997). The effects of non-periodic microstructure and defects on the compressive strength of two-dimensional cellular solids. *International Journal of Mechanical Sciences*, *39*(5), 549-563.

[38] Nakamoto, H., Adachi, T., & Araki, W. (2009). In-plane impact behavior of honeycomb structures randomly filled with rigid inclusions. *International Journal of Impact Engineering*, *36*(1), 73-80.

[39] Wang, A. J., & McDowell, D. L. (2003). Effects of defects on in-plane properties of periodic metal honeycombs. *International Journal of Mechanical Sciences*, *45*(11), 1799-1813.

[40] Zhang, X. C., Liu, Y., Wang, B., & Zhang, Z. M. (2010). Effects of defects on the in-plane dynamic crushing of metal honeycombs. *International Journal of Mechanical Sciences*, *52*(10), 1290-1298.

[41] Guo, X. E., & Gibson, L. J. (1999). Behavior of intact and damaged honeycombs: a finite element study. *International Journal of Mechanical Sciences*, *41*(1), 85-105.

[42] Li, K., Gao, X. L., & Subhash, G. (2005). Effects of cell shape and cell wall thickness variations on the elastic properties of two-dimensional cellular solids. *International Journal of Solids and Structures*, *42*(5), 1777-1795.

[43] Simone, A. E., & Gibson, L. J. (1998). The effects of cell face curvature and corrugations on the stiffness and strength of metallic foams. *Acta Materialia*, *46*(11), 3929-3935.

APPENDICES

Appendix A: APDL Batch for the finite element analysis of regular honeycomb structure

```
! This Batch finds the elastic modulus and Poisson's ratio of regular honeycomb
/UNITS,user
/FILNAM,Regular Honeycomb
/TITLE,Regular Honeycomb(1.01% missing cell walls) !% by mass density

/PREP7

ET,1,SOLID185,0                 !Element Type 3D 8-node solid
MP,EX,1,2.4e3                   !Material Properies
MP,PRXY,1,0.3
MP,GXY,1,2.4e3/(2*(1+0.30))     !(EX/2*(1+PRXY))

pi=3.14159265358979323846264 33
a= 16-(.8/sin (pi/3))           !length of cell wall edge of the honeycomb
t= 0.8                          ! Half of the thickness of the cell wall
a_=a+t/ (sin (pi/3))

H=((9*a_*sin(pi/3)+t)+(2*a_-a)*sin(pi/3))   !Height of the structure

yStrain=0.03                    !compressive displacement to be applied

!Keypoints to create one hexagon of regular honeycomb
k,1,a,0
k,2,a_,0
k,3,a_/2,a_*sin(pi/3),0
k,4,a/2,a*sin(pi/3),0
k,5,-a/2,a*sin(pi/3),0
k,6,-a_/2,a_*sin(pi/3),0
k,7,-a_,0
k,8,-a,0
k,9,-a/2,-a*sin(pi/3),0
k,10,-a_/2,-a_*sin(pi/3),0
k,11,a_/2,-a_*sin(pi/3),0
k,12,a/2,-a*sin(pi/3),0

!Create Areas for one cell
A,1,2,3,4
A,3,4,5,6
A,5,6,7,8
A,7,8,9,10
A,9,10,11,12
```

```
A,11,12,1,2

!Generate Pattern of Areas

AGEN,5,1,6,,0,(2*a+(t/sin(pi/3)))*sin(pi/3)+t,0
AGEN,5,1,6,,(a+(t/sin(pi/3)))*3/2,((2*a+(t/sin(pi/3)))*sin(pi/3)+t)/2,0

AGEN,5,7,12,,(a+(t/sin(pi/3)))*3/2,((2*a+(t/sin(pi/3)))*sin(pi/3)+t)/2,0
AGEN,5,13,18,,(a+(t/sin(pi/3)))*3/2,((2*a+(t/sin(pi/3)))*sin(pi/3)+t)/2,0
AGEN,3,19,24,,(a+(t/sin(pi/3)))*3/2,((2*a+(t/sin(pi/3)))*sin(pi/3)+t)/2,0

AGEN,2,31,36,,(a+(t/sin(pi/3)))*3/2,-(((2*a+(t/sin(pi/3)))*sin(pi/3)+t)/2),0
AGEN,3,37,42,,(a+(t/sin(pi/3)))*3/2,-(((2*a+(t/sin(pi/3)))*sin(pi/3)+t)/2),0
AGEN,2,43,48,,(a+(t/sin(pi/3)))*3/2,-(((2*a+(t/sin(pi/3)))*sin(pi/3)+t)/2),0


!Additional Keypoints to create Outside areas
K,277,-(2*a_-a),0,0

K,278,-(2*a_-a)/2,-(2*a_-a)*sin(pi/3),0
K,279,(2*a_-a)/2,-(2*a_-a)*sin(pi/3),0
K,280,a_+(a_-a)*cos(pi/3),-t,0

K,281,-(a_/2+t/sin(pi/3)),a_*sin(pi/3),0
K,282,-(2*a_-a),2*a_*sin(pi/3),0

!Outside areas

A,7,277,278,10,7
A,10,11,279,278,10
A,2,280,279,11,2
A,22,281,282,19,22
A,7,277,281,22,7

AGEN,4,142,,,0,2*a_*sin(pi/3),0
AGEN,4,143,,,0,2*a_*sin(pi/3),0

AGEN,2,143,,,9*a_-a-a_*cos(pi/3),a_*sin(pi/3),0
AGEN,4,150,,,0,2*a_*sin(pi/3),0

AGEN,2,142,,,9*a_-a-a_*cos(pi/3),-a_*sin(pi/3),0
AGEN,4,154,,,0,2*a_*sin(pi/3),0

K,339,(a_*sin(pi/3)+t)/tan(pi/3),9*a_*sin(pi/3)+t,0
K,340,-(a_*sin(pi/3)+t)/tan(pi/3),9*a_*sin(pi/3)+t,0
```

```
A,54,340,293,55,54
A,339,340,54,51,339

K,341,(3*a_-a)/2,(9*a_-a)*sin(pi/3),0,0
A,339,341,50,51,339

AGEN,3,159,,,3*a_,0,0
AGEN,2,160,,,3*a_,0,0

K,354,a+(3*a_-a)/2,(9*a_-a)*sin(pi/3),0
A,341,50,223,354,341
A,223,354,343,222,223
A,346,195,194,322,346
AGEN,2,165,,,3*a_,0,0
AGEN,2,164,,,3*a_,0,0

K,363,a_+(a_-a)*cos(pi/3)+a,-t,0
A,2,280,363,71,2
AGEN,3,140,,,3*a_,0,0
A,71,363,367,238,71

AGEN,2,141,,,3*a_,0,0
AGEN,2,169,,,3*a_,0,0
AGEN,2,172,,,3*a_,0,0
A,323,370,369,254,323

K,384,-(2*a_-a),0,10          !Keypoint for extrusion
L,384,277                     !Line of extrusion

EXTOPT,ESIZE,2,0
EXTOPT,ACLEAR,1

TYPE,1
MAT,1
REAL,1

!Extrude areas to Volumes
*DO,i,1,176,1
VDRAG,i,,,,,,547,,,,,,
*ENDDO

VSEL,all
VGLUE,all              !Glue all volumes

!Delete volumes as missing cell walls
```

```
VDELE,197
VDELE,302

!Enter Meshing of the model
MSHKEY,1                !Mapped Meshing
ESIZE,a/26

TYPE,1
MAT,1
REAL,1

VSEL,all
VMESH,all               !Volume mesh

SAVE

FINISH

/SOLUTION
ANTYPE,STATIC,NEW       !Static Analysis

!Apply Boundary conditions

NSEL,S,LOC,Y,-(2*a_-a)*sin(pi/3)          !Fix Bottom in Y direction
D,ALL,UY,0
NSEL,ALL

!Compressive displacement at top surface of the structure
NSEL,S,LOC,Y,125.50,125.51   !9*a_*sin(pi/3)+t
D,ALL,UY,-yStrain*H !dy i.e. % of total height of the structure
NSEL,ALL

NSEL,S,LOC,X,-(2*a_-a)      !Constrain X nodes for Symmetry
D,ALL,UX,0
NSEL,ALL

NSEL,S,LOC,Z,5              !Constrain halfway through Z direction
D,ALL,UZ,0
NSEL,ALL

SOLVE
SAVE
FINISH

/POST26
! Y direction Reaction forces at top nodes
```

```
NSEL,S,LOC,Y,125.50,125.51     !9*a_*sin(pi/3)+t
*GET,NODETOT,NODE,,COUNT
*GET,MINNODE,NODE,,NUM,MIN
NODENUM = MINNODE

RFORCE,3,NODENUM,F,Y,RFY
ADD,2,3,,,RFY,,,1

*DO,i,1,NODETOT-1,1

NODENUM=NDNEXT(NODENUM)

RFORCE,3,NODENUM,F,Y,RFY    !Variable name RFY
ADD,2,2,3,,RFY,,,1,1

*ENDDO
ALLSEL,ALL

!X Displacement of the extreme left nodes

NSEL,S,LOC,X,6*a_+a-a*cos(pi/3),8*a_-a
*GET,NODETOT,NODE,,COUNT
*GET,MINNODE,NODE,,NUM,MIN
NODENUM = MINNODE

NSOL,5,NODENUM,U,X,DISP1        !variable name DISP1
ADD,4,5,,,DISP1,,,1

*DO,i,1,NODETOT-1,1

NODENUM=NDNEXT(NODENUM)
NSOL,5,NODENUM,U,X,DISP1
ADD,4,4,5,,DISP1,,,1,1

*ENDDO

ALLSEL,ALL

ADD,4,4,,,DISP1,,,1/NODETOT,,,

!Z direction Displacement
NSEL,S,LOC,Z,10
*GET,NODETOT,NODE,,COUNT
*GET,MINNODE,NODE,,NUM,MIN
NODENUM = MINNODE
```

```
NSOL,7,NODENUM,U,Z,DISP2
ADD,6,7,,,DISP2,,,1

*DO,i,1,NODETOT-1,1

NODENUM=NDNEXT(NODENUM)
NSOL,7,NODENUM,U,Z,DISP2
ADD,6,6,7,,DISP2,,,1,1

*ENDDO

ALLSEL,ALL

ADD,6,6,,,DISP2,,,1/NODETOT,,,

*DIM,RFY,ARRAY,2
*DIM,TIME,ARRAY,2
*DIM,DISP1,ARRAY,2
*DIM,DISP2,ARRAY,2

VGET,RFY(1),2
VGET,TIME(1),1
VGET,DISP1(1),4
VGET,DISP2(1),6

FINISH

!Name the output file and format

/OUTPUT,Regular_1.01%missing cell walls results,TXT,,APPEND

*VWRITE
(10x,'Vol. of matrix',10x,'Vol %')

*VWRITE,VMATRIX,vol_per
(F18.9,' ',F18.9,' ')

*VWRITE
('TIME',10x,'RF_Y',10x,'STRESS_Y',10x,'DISP_X',10x,'DISP_Z',10x,'PR_XY',10x,'PR_
YZ')
*VWRITE,TIME(1),-RFY(1),-RFY(1)/((10*a_-2*a)*10),DISP1(1),DISP2(1),(-
DISP1(1)/(((10*a_-2*a))*(-yStrain))),(-DISP2(1)/(5*(-yStrain)))
(7(F12.5,2x))

/OUTPUT
/EOF
```

Appendix B: APDL Batch for finite element analysis of first order hierarchical honeycomb

```
! This Batch finds the elastic modulus and Poisson's ratio of 1st order Honeycomb
/UNITS,user
/FILNAM,1st order Honeycomb
/TITLE,1st Order Hierarchy (1.01% missing cell walls)

/PREP7
ET,1,SOLID185,0              !Element Type
MP,EX,1,2.4e3                !Material Properties
MP,PRXY,1,0.3
MP,GXY,1,2.4e3/(2*(1+0.30)) !(EX/2*(1+PRXY))

pi=3.14159265358979323846264 33
a=16-(.6/sin(pi/3))          !length of cell wall edge of regular oneycomb
t=1.2                        !Thickness of the cell walls
a_=a+t/sin(pi/3)
b=4.8-(.6/sin(pi/3))         !lenth of cell wall edge of 1st order hierachicy
b_=b+t/sin(pi/3)             !length of outer arm

H=5*(a+a_)*sin(pi/3)         !height of the structure

yStrain=0.03                 !compressive strain to be applied

!Keypoints for a single pattern
K,1,(a+a_+2*b)/2,0,0
K,2,(a+a_+b_)/2,b_*sin(pi/3),0
K,3,(a+a_+b)/2,b*sin(pi/3),0
K,4,(a+a_-b)/2,b*sin(pi/3),0
K,5,(a+a_-2*b_)/2,0,0
K,6,(a+a_-2*b)/2,0,0
K,7,(a+a_-b)/2,-b*sin(pi/3),0
K,8,(a+a_+b_)/2,-b_*sin(pi/3),0
K,9,(a+a_+b)/2,-b*sin(pi/3),0
K,10,(a+a_+2*b_)/2-((t*cos(pi/3))/(2*sin(pi/3))),t/2,0
K,11,(a+a_+2*b_)/2-((t*cos(pi/3))/(2*sin(pi/3))),-t/2,0


K,12,(a+a_-b)/2,b*sin(pi/3)+t,0
K,13,(a-(a+a_-2*b_)/2)/2+((a+a_-2*b_)/2),(a-(a+a_-2*b_)/2)*sin(pi/3),0

K,14,(a+a_-b)/2,-(b*sin(pi/3)+t),0
K,15,(a-(a+a_-2*b_)/2)/2+((a+a_-2*b_)/2),-((a-(a+a_-2*b_)/2)*sin(pi/3)),0
```

```
K,16,-((a+a_+2*b_)/2-((t*cos(pi/3))/(2*sin(pi/3)))),t/2,0
K,17,-((a+a_+2*b_)/2-((t*cos(pi/3))/(2*sin(pi/3)))),-t/2,0
K,18,-(a+a_+2*b)/2,0,0

K,19,-(a+a_-2*b_)/2,0,0
K,20,-(a+a_-2*b)/2,0,0
K,21,-(a+a_-b)/2,b*sin(pi/3)+t,0
K,22,-((a-(a+a_-2*b_)/2)/2+((a+a_-2*b_)/2)),(a-(a+a_-2*b_)/2)*sin(pi/3),0

K,23,-(a+a_-b)/2,-b*sin(pi/3),0
K,24,-(a+a_-b)/2,-(b*sin(pi/3)+t),0
K,25,-((a-(a+a_-2*b_)/2)/2+((a+a_-2*b_)/2)),-((a-(a+a_-2*b_)/2)*sin(pi/3)),0


K,26,-(a+a_+b_)/2,-b_*sin(pi/3),0
K,27,-(a+a_+b)/2,-b*sin(pi/3),0
K,28,-(a+a_+b_)/2,b_*sin(pi/3),0
K,29,-(a+a_+b)/2,b*sin(pi/3),0

K,30,-(a+a_-b)/2,b*sin(pi/3),0

!create areas of a single pattern
A,1,10,2,3,1
A,2,3,4,12,2
A,4,13,5,6,4
A,5,6,7,15,5
A,7,9,8,14,7
A,9,8,11,1,9
A,20,19,25,23,20
A,23,24,26,27,23
A,26,27,18,17,26
A,16,18,29,28,16
A,28,29,30,21,28
A,30,22,19,20,30

K,31,1.5*(a+a_)/2,t/2,0
K,32,1.5*(a+a_)/2,0,0
K,33,1.5*(a+a_)/2,-t/2,0
K,34,-1.5*(a+a_)/2,t/2,0
K,35,-1.5*(a+a_)/2,0,0
K,36,-1.5*(a+a_)/2,-t/2,0
A,1,10,31,32,1
A,1,11,33,32,1
A,18,17,36,35,18
A,18,16,34,35,18
```

```
AGEN,2,1,3,,-(3/4)*(a+a_),-((a+a_)/2)*sin(pi/3),0
AGEN,2,13,,,-(3/4)*(a+a_),-((a+a_)/2)*sin(pi/3),0

AGEN,2,10,12,,(3/4)*(a+a_),-((a+a_)/2)*sin(pi/3),0
AGEN,2,16,,,(3/4)*(a+a_),-((a+a_)/2)*sin(pi/3),0

AGEN,2,4,6,,-(3/4)*(a+a_),((a+a_)/2)*sin(pi/3),0
AGEN,2,14,,,-(3/4)*(a+a_),((a+a_)/2)*sin(pi/3),0

AGEN,2,7,9,,(3/4)*(a+a_),((a+a_)/2)*sin(pi/3),0
AGEN,2,15,,,(3/4)*(a+a_),((a+a_)/2)*sin(pi/3),0

A,4,12,78,79,4
A,4,13,80,79,4
A,7,15,55,54,7
A,7,14,56,54,7
A,65,66,21,30,65
A,30,22,69,65,30
A,23,24,43,41,23
A,23,25,42,41,23

AGEN,3,1,40,,2*1.5*(a+a_)/2,0,0
AGEN,5,1,120,,0,t+2*a*sin(pi/3),0


K,1321,0,0,0
K,1322,0,0,10
L,1321,1322



EXTOPT,ESIZE,2,0
EXTOPT,ACLEAR,1

TYPE,1
MAT,1
REAL,1

*DO,i,1,600,1
VDRAG,i,,,,,,1861,,,,,,
*ENDDO

VSEL,all
VGLUE,all
```

```
VDELE,813
VDELE,814
VDELE,887
VDELE,1019
VDELE,1020
VDELE,1113
VDELE,1114
VDELE,913



MSHKEY,1
ESIZE,a/21


TYPE,1
MAT,1
REAL,1

VSEL,all
VMESH,all

SAVE
FINISH

/SOLUTION
ANTYPE,STATIC,NEW

!Apply Boundary conditions

NSEL,S,LOC,Y,-((a+a_)/2)*sin(pi/3)
D,ALL,UY,0
NSEL,ALL

NSEL,S,LOC,Y,124.70,124.71   !4.5*(a+a_)*sin(pi/3)
D,ALL,UY,-yStrain*H          !dy i.e. % of total height of the structure
NSEL,ALL

NSEL,S,LOC,X,-1.5*(a+a_)/2
D,ALL,UX,0
NSEL,ALL

NSEL,S,LOC,Z,5
D,ALL,UZ,0
NSEL,ALL
```

```
SOLVE
SAVE
FINISH

/POST26

NSEL,S,LOC,Y,124.70,124.71     !9*a_*sin(pi/3)+t
*GET,NODETOT,NODE,,COUNT
*GET,MINNODE,NODE,,NUM,MIN
NODENUM = MINNODE

RFORCE,3,NODENUM,F,Y,RFY
ADD,2,3,,,RFY,,,1

*DO,i,1,NODETOT-1,1

NODENUM=NDNEXT(NODENUM)

RFORCE,3,NODENUM,F,Y,RFY
ADD,2,2,3,,RFY,,,1,1

*ENDDO
ALLSEL,ALL

NSEL,S,LOC,X,7.5*((a+a_)/2)
*GET,NODETOT,NODE,,COUNT
*GET,MINNODE,NODE,,NUM,MIN
NODENUM = MINNODE

NSOL,5,NODENUM,U,X,DISP1        !here the variable name should be disp1
ADD,4,5,,,DISP1,,,1

*DO,i,1,NODETOT-1,1

NODENUM=NDNEXT(NODENUM)
NSOL,5,NODENUM,U,X,DISP1
ADD,4,4,5,,DISP1,,,1,1

*ENDDO

ALLSEL,ALL
ADD,4,4,,,DISP1,,,1/NODETOT,,,

NSEL,S,LOC,Z,10
*GET,NODETOT,NODE,,COUNT
*GET,MINNODE,NODE,,NUM,MIN
```

```
NODENUM = MINNODE

NSOL,7,NODENUM,U,Z,DISP2
ADD,6,7,,,DISP2,,,1

*DO,i,1,NODETOT-1,1

NODENUM=NDNEXT(NODENUM)
NSOL,7,NODENUM,U,Z,DISP2
ADD,6,6,7,,DISP2,,,1,1

*ENDDO

ALLSEL,ALL
ADD,6,6,,,DISP2,,,1/NODETOT,,,

*DIM,RFY,ARRAY,2
*DIM,TIME,ARRAY,2
*DIM,DISP1,ARRAY,2
*DIM,DISP2,ARRAY,2

VGET,RFY(1),2
VGET,TIME(1),1
VGET,DISP1(1),4
VGET,DISP2(1),6

/OUTPUT,1st order_1.01%missing _Results,TXT,,APPEND

*VWRITE
(10x,'Vol. of matrix',10x,'Vol %')

*VWRITE,VMATRIX,vol_per
(F18.9,' ',F18.9,' ')

*VWRITE
('TIME',10x,'RF_Y',10x,'STRESS_Y',10x,'DISP_X',10x,'DISP_Z',10x,'PR_XY',10x,'PR_
YZ')
*VWRITE,TIME(1),-RFY(1),-RFY(1)/((9*(a+a_)/2)*10),DISP1(1),DISP2(1),(-
DISP1(1)/(((9*(a+a_)/2))*(-yStrain))),(-DISP2(1)/(5*(-yStrain)))
(7(F12.5,2x))

/OUTPUT
/EOF
```

Appendix C: APDL Batch for finite element analysis of second order hierarchical honeycomb

```
! This Batch finds the transverse elastic modulus and Poisson's ratio of 1st order
!Honeycomb
/UNITS,user
/FILNAM,2nd order Honeycomb
/TITLE,2nd Order Hierarchy


/PREP7
ET,1,SOLID185,0
MP,EX,1,2.4e3
MP,PRXY,1,0.3
MP,GXY,1,2.4e3/(2*(1+0.30))

pi=3.14159265358979323846264 33
a=16-(.4/sin(pi/3))     !Inner arm of regular hexagon
t=.8                    !thickness of the cell wall
a_=a+t/sin(pi/3)        !Outer arm of regular hexagon
b=4.8-(.4/sin(pi/3))    !Inner arm of first order hexagon
b_=b+t/sin(pi/3)        !outer arm of first order hexagon
c=2-(.4/sin(pi/3))      !Inner arm of second order hexagon
c_=c+t/sin(pi/3)        !outer arm of second order hexagon

L=10*((a+a_)/2)*sin(pi/3) !Length of the structure

xStrain=0.03            !Strain to be applied


K,1,b+c+a_,0,0
K,2,b+c+2*a_-a-c_*cos(pi/3),c_*sin(pi/3),0
K,3,b+c+a_-c*cos(pi/3),c*sin(pi/3),0
K,4,b+a_-c*cos(pi/3),c*sin(pi/3),0
K,5,b+c+2*a_-a-2*c_,0,0
K,6,b+c+a_-2*c,0,0
K,7,b+a_-c*cos(pi/3),-c*sin(pi/3),0
K,8,(a+a_)/2+(b+b_)/2+(c+c_)/2+(t*cos(pi/3))/(2*sin(pi/3)),t/2,0
K,9,(a+a_)/2+(b+b_)/2+(c+c_)/2+(t*cos(pi/3))/(2*sin(pi/3)),-t/2,0
K,10,(5*a_)/2-(3*a)/2+b+c-(3*c_)/2,c_*sin(pi/3),0
K,11,(a+a_+2*b)/2-(c+t/(2*sin(pi/3)))*cos(pi/3),(c+t/(2*sin(pi/3)))*sin(pi/3),0
K,12,(5*a_)/2-(3*a)/2+b+c-(3*c_)/2,-c_*sin(pi/3),0
K,13,(a+a_+2*b)/2-(c+t/(2*sin(pi/3)))*cos(pi/3),-(c+t/(2*sin(pi/3)))*sin(pi/3),0
K,14,b+c+2*a_-a-c_*cos(pi/3),-c_*sin(pi/3),0
K,15,b+c+a_-c*cos(pi/3),-c*sin(pi/3),0
```

```
A,1,8,2,3,1
A,2,3,4,10,2
A,4,11,5,6,4
A,5,6,7,13,5
A,7,15,14,12,7
A,15,14,9,1,15

AGEN,2,1,6,,-(((b+b_)/2)*cos(pi/3)+(b+b_)/2),((b+b_)/2)*sin(pi/3),0
AGEN,2,1,6,,-(((b+b_)/2)*cos(pi/3)+(b+b_)/2),-((b+b_)/2)*sin(pi/3),0

K,46,-(b+c+a_),0,0
K,47,-(b+c+2*a_-a-c_*cos(pi/3)),c_*sin(pi/3),0
K,48,-(b+c+a_-c*cos(pi/3)),c*sin(pi/3),0
K,49,-(b+a_-c*cos(pi/3)),c*sin(pi/3),0
K,50,-(b+c+2*a_-a-2*c_),0,0
K,51,-(b+c+a_-2*c),0,0
K,52,-(b+a_-c*cos(pi/3)),-c*sin(pi/3),0
K,53,-((a+a_)/2+(b+b_)/2+(c+c_)/2+(t*cos(pi/3))/(2*sin(pi/3))),t/2,0
K,54,-((a+a_)/2+(b+b_)/2+(c+c_)/2+(t*cos(pi/3))/(2*sin(pi/3))),-t/2,0
K,55,-((5*a_)/2-(3*a)/2+b+c-(3*c_)/2),c_*sin(pi/3),0
K,56,-((a+a_+2*b)/2-(c+t/(2*sin(pi/3)))*cos(pi/3)),(c+t/(2*sin(pi/3)))*sin(pi/3),0
K,57,-((5*a_)/2-(3*a)/2+b+c-(3*c_)/2),-c_*sin(pi/3),0
K,58,-((a+a_+2*b)/2-(c+t/(2*sin(pi/3)))*cos(pi/3)),-(c+t/(2*sin(pi/3)))*sin(pi/3),0
K,59,-(b+c+2*a_-a-c_*cos(pi/3)),-c_*sin(pi/3),0
K,60,-(b+c+a_-c*cos(pi/3)),-c*sin(pi/3),0

A,50,51,52,58,50
A,52,57,59,60,52
A,59,60,46,54,59
A,46,53,47,48,46
A,47,48,49,55,47
A,49,56,50,51,49


AGEN,2,19,24,,(((b+b_)/2)*cos(pi/3)+(b+b_)/2),((b+b_)/2)*sin(pi/3),0
AGEN,2,19,24,,(((b+b_)/2)*cos(pi/3)+(b+b_)/2),-((b+b_)/2)*sin(pi/3),0

K,91,b*cos(pi/3)+(a+a_)/2,b*sin(pi/3),0
K,92,((b+b_)/2)*cos(pi/3)+(a+a_)/2,((b+b_)/2)*sin(pi/3),0
K,93,b_*cos(pi/3)+(a+a_)/2,b_*sin(pi/3),0
K,94,b*cos(pi/3)+(a+a_)/2,-b*sin(pi/3),0
K,95,((b+b_)/2)*cos(pi/3)+(a+a_)/2,-((b+b_)/2)*sin(pi/3),0
K,96,b_*cos(pi/3)+(a+a_)/2,-b_*sin(pi/3),0
K,97,(a+a_-2*b)/2,0,0
K,98,(a+a_-2*b_)/2,0,0
K,99,a-b,0,0
```

```
K,100,-(b*cos(pi/3)+(a+a_)/2),b*sin(pi/3),0
K,101,-(((b+b_)/2)*cos(pi/3)+(a+a_)/2),((b+b_)/2)*sin(pi/3),0
K,102,-(b_*cos(pi/3)+(a+a_)/2),b_*sin(pi/3),0
K,103,-(b*cos(pi/3)+(a+a_)/2),-b*sin(pi/3),0
K,104,-(((b+b_)/2)*cos(pi/3)+(a+a_)/2),-((b+b_)/2)*sin(pi/3),0
K,105,-(b_*cos(pi/3)+(a+a_)/2),-b_*sin(pi/3),0
K,106,-(a+a_-2*b)/2,0,0
K,107,-(a+a_-2*b_)/2,0,0
K,108,b-a,0,0

A,1,3,2,8,1
A,2,3,4,10,2
A,4,11,5,6,4
A,5,6,7,13,5
A,7,12,14,15,7
A,14,15,1,9,14

A,91,92,4,11,91
A,4,10,93,92,4
A,91,92,16,30,91
A,92,93,17,16,92
A,16,17,18,19,16
A,18,19,20,21,18
A,20,22,23,24,20
A,23,24,25,26,23
A,25,27,28,29,25
A,27,28,30,16,27

A,31,32,33,34,31
A,33,34,35,36,33
A,35,37,38,39,35
A,38,39,40,41,38
A,40,44,43,42,40
A,42,43,45,31,42

A,32,94,95,31,32
A,31,95,96,45,31
A,94,13,7,95,94
A,95,7,12,96,95

A,25,26,98,99,25
A,25,99,97,29,25
A,98,99,35,37,98
```

```
A,97,99,35,36,97

A,75,61,62,73,75
A,61,62,63,64,61
A,63,65,66,67,63
A,66,67,68,69,66
A,68,70,71,72,68

A,49,56,50,51,49
A,50,51,52,58,50
A,52,60,59,57,52
A,60,59,54,46,60
A,46,48,47,53,46
A,48,49,55,47,48

A,90,88,77,76,90
A,76,77,78,79,76
A,78,80,81,82,78
A,81,82,83,84,81
A,83,85,86,87,83
A,86,87,88,89,86

A,63,64,107,108,63
A,63,65,106,108,63
A,106,108,88,89,106
A,88,90,107,108,88
A,102,101,68,70,102
A,101,100,69,68,101
A,102,101,49,55,102
A,49,56,100,101,49

A,103,104,52,58,103
A,104,105,57,52,104
A,103,85,83,104,103
A,104,105,84,83,104



AGEN,3,1,60,,(3/2)*(a+a_),0,0
AGEN,5,1,180,,0,2*((a+a_)/2)*sin(pi/3),0


AGEN,2,1,18,,-(((a+a_-
2*b_)/2)+b_+(a+t/(2*sin(pi/3)))*cos(pi/3)),(a+t/(2*sin(pi/3)))*sin(pi/3),0
AGEN,2,37,48,,-(((a+a_-
2*b_)/2)+b_+(a+t/(2*sin(pi/3)))*cos(pi/3)),(a+t/(2*sin(pi/3)))*sin(pi/3),0
```

```
AGEN,2,19,36,,((a+a_-
2*b_)/2)+b_+(a+t/(2*sin(pi/3)))*cos(pi/3),((a+t/(2*sin(pi/3)))*sin(pi/3)),0
AGEN,2,49,60,,((a+a_-
2*b_)/2)+b_+(a+t/(2*sin(pi/3)))*cos(pi/3),((a+t/(2*sin(pi/3)))*sin(pi/3)),0


AGEN,3,901,960,,(3/2)*(a+a_),0,0
AGEN,4,901,1080,,0,2*((a+a_)/2)*sin(pi/3),0


!Bottom and top

AGEN,2,1,3,,-(((a+a_-2*b_)/2)+b_+(a+t/(2*sin(pi/3)))*cos(pi/3)),-
((a+t/(2*sin(pi/3)))*sin(pi/3)),0
AGEN,2,7,12,,-(((a+a_-2*b_)/2)+b_+(a+t/(2*sin(pi/3)))*cos(pi/3)),-
((a+t/(2*sin(pi/3)))*sin(pi/3)),0
AGEN,2,37,40,,-(((a+a_-2*b_)/2)+b_+(a+t/(2*sin(pi/3)))*cos(pi/3)),-
((a+t/(2*sin(pi/3)))*sin(pi/3)),0
AGEN,2,45,46,,-(((a+a_-2*b_)/2)+b_+(a+t/(2*sin(pi/3)))*cos(pi/3)),-
((a+t/(2*sin(pi/3)))*sin(pi/3)),0

AGEN,2,22,30,,((a+a_-2*b_)/2)+b_+(a+t/(2*sin(pi/3)))*cos(pi/3),-
((a+t/(2*sin(pi/3)))*sin(pi/3)),0
AGEN,2,49,50,,((a+a_-2*b_)/2)+b_+(a+t/(2*sin(pi/3)))*cos(pi/3),-
((a+t/(2*sin(pi/3)))*sin(pi/3)),0
AGEN,2,53,56,,((a+a_-2*b_)/2)+b_+(a+t/(2*sin(pi/3)))*cos(pi/3),-
((a+t/(2*sin(pi/3)))*sin(pi/3)),0

AGEN,3,1621,1650,,(3/2)*(a+a_),0,0
AGEN,2,1453,1458,,0,2*((a+a_)/2)*sin(pi/3),0
AGEN,2,1444,1446,,0,2*((a+a_)/2)*sin(pi/3),0
AGEN,2,1463,1466,,0,2*((a+a_)/2)*sin(pi/3),0
AGEN,2,1469,1470,,0,2*((a+a_)/2)*sin(pi/3),0

AGEN,2,1483,1488,,0,2*((a+a_)/2)*sin(pi/3),0
AGEN,2,1471,1473,,0,2*((a+a_)/2)*sin(pi/3),0
AGEN,2,1497,1500,,0,2*((a+a_)/2)*sin(pi/3),0
AGEN,2,1491,1492,,0,2*((a+a_)/2)*sin(pi/3),0
AGEN,3,1711,1740,,(3/2)*(a+a_),0,0

A,3350,3352,3391,3389,3350
A,3430,3469,3467,3428,3430
A,3508,3547,3545,3506,3508
A,80,3364,3362,78,80
```

A,78,79,3363,3362,78
A,3409,3411,44,40,3409
A,3409,3410,41,40,3409
A,3440,3442,188,186,3440
A,3440,186,187,3441,3440
A,148,149,3488,3487,148
A,148,150,3489,3487,148
A,294,296,3520,3518,294
A,3518,3519,295,294,3518
A,3565,3566,257,256,3565
A,256,258,3567,3565,256
A,73,74,1661,1660,73
A,73,75,1662,1660,73
A,20,21,1726,1725,20
A,20,22,1727,1725,20
A,181,183,1806,1804,181
A,181,182,1805,1804,181
A,128,130,1871,1869,128
A,128,129,1870,1869,128
A,289,291,1950,1948,289
A,289,290,1949,1948,289
A,236,237,2014,2013,236
A,236,238,2015,2013,236
A,1622,1635,1700,1701,1622
A,1622,1624,1704,1701,1622
A,1766,1779,1844,1845,1766
A,1766,1768,1848,1845,1766
A,1910,1923,1988,1989,1910
A,1910,1912,1992,1989,1910
A,1,9,161,162,1
A,1,8,165,162,1
A,110,123,269,270,110
A,110,112,273,270,110
A,1642,404,402,1640,1642
A,1640,402,403,1641,1640
A,1720,1722,366,364,1720
A,1720,1721,365,364,1720
A,1784,1786,512,510,1784
A,1784,1785,511,510,1784
A,1864,1866,474,472,1864
A,1864,1865,473,472,1864
A,1928,1930,620,618,1928
A,1928,1929,619,618,1928
A,2008,2010,582,580,2008
A,2008,2009,581,580,2008
A,326,339,485,486,326

A,326,328,489,486,326
A,434,447,593,594,434
A,434,436,597,594,434
A,397,398,2093,2092,397
A,397,399,2094,2092,397
A,344,346,2159,2157,344
A,344,345,2158,2157,344
A,505,507,2238,2236,505
A,505,506,2237,2236,505
A,452,454,2303,2301,452
A,452,453,2302,2301,452
A,613,615,2382,2380,613
A,613,614,2381,2380,613
A,560,562,2447,2445,560
A,560,561,2446,2445,560
A,2054,2067,2132,2133,2054
A,2054,2056,2136,2133,2054
A,2198,2211,2276,2277,2198
A,2198,2200,2280,2277,2198
A,2342,2355,2420,2421,2342
A,2342,2344,2424,2421,2342
A,2072,2074,728,726,2072
A,2072,726,727,2073,2072
A,2152,2153,689,688,2152
A,2152,2154,690,688,2152
A,2216,2218,836,834,2216
A,2216,2217,835,834,2216
A,2296,2297,797,796,2296
A,2296,2298,798,796,2296
A,2360,2362,944,942,2360
A,2360,2361,943,942,2360
A,2440,2441,905,904,2440
A,2440,2442,906,904,2440
A,650,663,809,810,650
A,650,652,813,810,650
A,758,771,917,918,758
A,758,760,921,918,758
A,721,722,2525,2524,721
A,721,723,2526,2524,721
A,668,670,2591,2589,668
A,668,669,2590,2589,668
A,829,830,2669,2668,829
A,829,831,2670,2668,829
A,776,778,2735,2733,776
A,776,777,2734,2733,776
A,937,938,2813,2812,937

A,937,939,2814,2812,937
A,884,886,2879,2877,884
A,884,885,2878,2877,884
A,2486,2488,2568,2565,2486
A,2486,2499,2564,2565,2486
A,2630,2643,2708,2709,2630
A,2630,2632,2712,2709,2630
A,2774,2787,2852,2853,2774
A,2774,2776,2856,2853,2774
A,2504,2506,1052,1050,2504
A,2504,2505,1051,1050,2504
A,2584,2586,1014,1012,2584
A,2584,2585,1013,1012,2584
A,2648,2650,1160,1158,2648
A,2648,2649,1159,1158,2648
A,2728,2729,1121,1120,2728
A,2728,2730,1122,1120,2728
A,2792,2794,1268,1266,2792
A,2792,2793,1267,1266,2792
A,2872,2873,1229,1228,2872
A,2872,2874,1230,1228,2872
A,974,976,1137,1134,974
A,974,987,1133,1134,974
A,1082,1084,1245,1242,1082
A,1082,1095,1241,1242,1082
A,1045,1046,2957,2956,1045
A,1045,1047,2958,2956,1045
A,992,994,3023,3021,992
A,992,993,3022,3021,992
A,1153,1154,3101,3100,1153
A,1153,1155,3102,3100,1153
A,1100,1102,3167,3165,1100
A,1100,1101,3166,3165,1100
A,1261,1262,3245,3244,1261
A,1261,1263,3246,3244,1261
A,1208,1210,3311,3309,1208
A,1208,1209,3310,3309,1208
A,2918,2931,2996,2997,2918
A,2918,2920,3000,2997,2918
A,3062,3075,3140,3141,3062
A,3062,3064,3144,3141,3062
A,3206,3219,3284,3285,3206
A,3206,3208,3288,3285,3206
A,2936,2938,1376,1374,2936
A,2936,2937,1375,1374,2936
A,3016,3017,1337,1336,3016

```
A,3016,3018,1338,1336,3016
A,3080,3081,1483,1482,3080
A,3080,3082,1484,1482,3080
A,3160,3161,1445,1444,3160
A,3160,3162,1446,1444,3160
A,3224,3226,1592,1590,3224
A,3224,3225,1591,1590,3224
A,3304,3305,1553,1552,3304
A,3304,3306,1554,1552,3304
A,1298,1300,1461,1458,1298
A,1298,1311,1457,1458,1298
A,1406,1408,1569,1566,1406
A,1406,1419,1565,1566,1406
A,1369,1370,3593,3592,1369
A,1369,1371,3594,3592,1369
A,1316,1318,3626,3624,1316
A,1316,1317,3625,3624,1316
A,1477,1478,3671,3670,1477
A,1477,1479,3672,3670,1477
A,1424,1426,3704,3702,1424
A,1424,1425,3703,3702,1424
A,1585,1586,3749,3748,1585
A,1585,1587,3750,3748,1585
A,1532,1534,3782,3780,1532
A,1532,1533,3781,3780,1532
A,3606,3605,3645,3644,3606
A,3684,3683,3723,3722,3684
A,3762,3761,3801,3800,3762


K,3817,-(3/4)*(a+a_),0,0
K,3818,-(3/4)*(a+a_),t/2,0
K,3819,-(3/4)*(a+a_),-t/2,0


K,3820,-(3/4)*(a+a_),2*((a+a_)/2)*sin(pi/3),0
K,3821,-(3/4)*(a+a_),(t/2)+2*((a+a_)/2)*sin(pi/3),0
K,3822,-(3/4)*(a+a_),(-t/2)+2*((a+a_)/2)*sin(pi/3),0


K,3823,-(3/4)*(a+a_),4*((a+a_)/2)*sin(pi/3),0
K,3824,-(3/4)*(a+a_),(t/2)+4*((a+a_)/2)*sin(pi/3),0
K,3825,-(3/4)*(a+a_),(-t/2)+4*((a+a_)/2)*sin(pi/3),0

K,3826,-(3/4)*(a+a_),6*((a+a_)/2)*sin(pi/3),0
K,3827,-(3/4)*(a+a_),(t/2)+6*((a+a_)/2)*sin(pi/3),0
```

```
K,3828,-(3/4)*(a+a_),(-t/2)+6*((a+a_)/2)*sin(pi/3),0

K,3829,-(3/4)*(a+a_),8*((a+a_)/2)*sin(pi/3),0
K,3830,-(3/4)*(a+a_),(t/2)+8*((a+a_)/2)*sin(pi/3),0
K,3831,-(3/4)*(a+a_),(-t/2)+8*((a+a_)/2)*sin(pi/3),0


K,3832,5*(3/4)*(a+a_),0,0
K,3833,5*(3/4)*(a+a_),t/2,0
K,3834,5*(3/4)*(a+a_),-t/2,0


K,3835,5*(3/4)*(a+a_),2*((a+a_)/2)*sin(pi/3),0
K,3836,5*(3/4)*(a+a_),(t/2)+2*((a+a_)/2)*sin(pi/3),0
K,3837,5*(3/4)*(a+a_),(-t/2)+2*((a+a_)/2)*sin(pi/3),0


K,3838,5*(3/4)*(a+a_),4*((a+a_)/2)*sin(pi/3),0
K,3839,5*(3/4)*(a+a_),(t/2)+4*((a+a_)/2)*sin(pi/3),0
K,3840,5*(3/4)*(a+a_),(-t/2)+4*((a+a_)/2)*sin(pi/3),0

K,3841,5*(3/4)*(a+a_),6*((a+a_)/2)*sin(pi/3),0
K,3842,5*(3/4)*(a+a_),(t/2)+6*((a+a_)/2)*sin(pi/3),0
K,3843,5*(3/4)*(a+a_),(-t/2)+6*((a+a_)/2)*sin(pi/3),0

K,3844,5*(3/4)*(a+a_),8*((a+a_)/2)*sin(pi/3),0
K,3845,5*(3/4)*(a+a_),(t/2)+8*((a+a_)/2)*sin(pi/3),0
K,3846,5*(3/4)*(a+a_),(-t/2)+8*((a+a_)/2)*sin(pi/3),0

A,46,54,3819,3817,46
A,46,53,3818,3817,46
A,378,377,3822,3820,378
A,378,381,3821,3820,378
A,702,701,3825,3823,702
A,702,705,3824,3823,702
A,1026,1025,3828,3826,1026
A,1026,1029,3827,3826,1026
A,1350,1349,3831,3829,1350
A,1350,1353,3830,3829,1350

A,218,220,3833,3832,218
A,218,231,3834,3832,218
A,542,555,3837,3835,542
A,542,544,3836,3835,542
A,866,879,3840,3838,866
A,866,868,3839,3838,866
```

```
A,1190,1203,3843,3841,1190
A,1190,1192,3842,3841,1190
A,1514,1527,3846,3844,1514
A,1514,1516,3845,3844,1514



K,3847,0,0,0
K,3848,0,0,10
L,3847,3848

EXTOPT,ESIZE,2,0
EXTOPT,ACLEAR,1

TYPE,1
MAT,1
REAL,1

*DO,i,1,1990,1
VDRAG,i,,,,,,5907,,,,,,
*ENDDO


VSEL,all
VGLUE,all

VDELE,2279
VDELE,2325
VDELE,2446
VDELE,2554
VDELE,2608
VDELE,2896
VDELE,3064
VDELE,3274
VDELE,3275
VDELE,3352
VDELE,3353
VDELE,3390
VDELE,3391
VDELE,3447
VDELE,3451
VDELE,3483
VDELE,3487
VDELE,3609
VDELE,3613
VDELE,3635
```

```
VDELE,3640

MSHKEY,1
ESIZE,a/18

TYPE,1
MAT,1
REAL,1

VSEL,all
VMESH,all

SAVE
FINISH

/SOLUTION
ANTYPE,STATIC,NEW

!Apply Boundary conditions

NSEL,S,LOC,Y,-((a+a_)/2)*sin(pi/3)
D,ALL,UY,0
NSEL,ALL

!NSEL,S,LOC,X,9*((a+a_)/2)*sin(pi/3)
NSEL,S,LOC,X,124.70,124.71
D,ALL,UY,-xStrain*L
NSEL,ALL

NSEL,S,LOC,X,-1.5*(a+a_)/2
D,ALL,UX,0
NSEL,ALL

NSEL,S,LOC,Z,5
D,ALL,UZ,0
NSEL,ALL

SOLVE
SAVE
FINISH

/POST26

NSEL,S,LOC,Y,124.70,124.71     !9*a_*sin(pi/3)+t
*GET,NODETOT,NODE,,COUNT
*GET,MINNODE,NODE,,NUM,MIN
```

```
NODENUM = MINNODE

RFORCE,3,NODENUM,F,Y,RFY
ADD,2,3,,,RFY,,,1

*DO,i,1,NODETOT-1,1

NODENUM=NDNEXT(NODENUM)

RFORCE,3,NODENUM,F,Y,RFY
ADD,2,2,3,,RFY,,,1,1

*ENDDO
ALLSEL,ALL

NSEL,S,LOC,X,7.5*(a+a_)/2                    6*a_+a*cos(pi/3),8*a_-a
*GET,NODETOT,NODE,,COUNT
*GET,MINNODE,NODE,,NUM,MIN
NODENUM = MINNODE

NSOL,5,NODENUM,U,X,DISP1        !here the variable name should be disp1
ADD,4,5,,,DISP1,,,1

*DO,i,1,NODETOT-1,1

NODENUM=NDNEXT(NODENUM)
NSOL,5,NODENUM,U,X,DISP1
ADD,4,4,5,,DISP1,,,1,1

*ENDDO

ALLSEL,ALL

ADD,4,4,,,DISP1,,,1/NODETOT,,,

NSEL,S,LOC,Z,10
*GET,NODETOT,NODE,,COUNT
*GET,MINNODE,NODE,,NUM,MIN
NODENUM = MINNODE

NSOL,7,NODENUM,U,Z,DISP2
ADD,6,7,,,DISP2,,,1

*DO,i,1,NODETOT-1,1

NODENUM=NDNEXT(NODENUM)
```

```
NSOL,7,NODENUM,U,Z,DISP2
ADD,6,6,7,,DISP2,,,1,1

*ENDDO

ALLSEL,ALL

ADD,6,6,,,DISP2,,,1/NODETOT,,,

*DIM,RFY,ARRAY,2
*DIM,TIME,ARRAY,2
*DIM,DISP1,ARRAY,2
*DIM,DISP2,ARRAY,2

VGET,RFY(1),2
VGET,TIME(1),1
VGET,DISP1(1),4
VGET,DISP2(1),6

/OUTPUT,2nd order_1.01%missing _Results,TXT,,APPEND

*VWRITE
(10x,'Vol. of matrix',10x,'Vol %')

*VWRITE,VMATRIX,vol_per
(F18.9,' ',F18.9,' ')

*VWRITE
('TIME',10x,'RF_Y',10x,'STRESS_Y',10x,'DISP_X',10x,'DISP_Z',10x,'PR_XY',10x,'PR_
YZ')
*VWRITE,TIME(1),-RFY(1),-RFY(1)/((9*(a+a_)/2)*10),DISP1(1),DISP2(1),(-
DISP1(1)/(((9*(a+a_)/2))*(-xStrain))),(-DISP2(1)/(5*(-xStrain)))
(7(F12.5,2x))

/OUTPUT
/EOF
```

Appendix D: MATLAB code to calculate the elastic modulus of experimental data

```
clear all
close all
clc

filename = '2nd order_intact.txt';
filename2 = '2nd order_intact';

depth = 10/1000;   %in meters
width = 129/1000;   %in meters

gauge_length = 142.18/1000;    %in m
range = 200:500;

temp = csvread(filename,7,0);
time = temp(:,1);   %sec
disp = -temp(:,2)/1000;   %in then m
force = -temp(:,3);   %N

area = 1440/1e6%depth*width;  %m^2
stress = force/area;   %in Pa
strain = disp/(gauge_length);    %in mm/mm
strain = strain - strain(1);

[coeff] = polyfit(strain(range),stress(range),1);

E = coeff(1)

strain_plus = stress/E + 0.002;

for i=1:length(strain)
    flip = sign(stress(i)-(E*(strain(i)-.002)+coeff(2)));
    if flip ~= 1
        break
    end
end

plot(strain,stress/1e6,strain,(E*strain+coeff(2))/1e6)
axis([0 0.05 0 .05])
xlabel('Strain (mm/mm)')
ylabel('Stress (MPa)')
saveas(gcf,filename2,'fig')
saveas(gcf,filename2,'jpeg')
```